

**INORGANIC
CHEMISTRY**
FRONTIERS



Hydrogenation Reactions Catalyzed by HN(CH₂CH₂PR₂)₂-Ligated Copper Complexes

Journal:	<i>Inorganic Chemistry Frontiers</i>
Manuscript ID	QI-RES-06-2021-000776.R1
Article Type:	Research Article
Date Submitted by the Author:	15-Aug-2021
Complete List of Authors:	Ekanayake, Dewmi; University of Cincinnati, Department of Chemistry Chakraborty, Arundhoti ; University of Cincinnati, Department of Chemistry Krause, Jeanette; University of Cincinnati, Chemistry Guan, Hairong; University of Cincinnati,

SCHOLARONE™
Manuscripts

Hydrogenation Reactions Catalyzed by $\text{HN}(\text{CH}_2\text{CH}_2\text{PR}_2)_2$ -Ligated Copper Complexes

*Dewmi A. Ekanayake, Arundhoti Chakraborty, Jeanette A. Krause, and Hairong Guan**

Department of Chemistry, University of Cincinnati, P.O. Box 210172, Cincinnati, Ohio 45221-0172, United States

*E-mail: hairong.guan@uc.edu; Tel: +1-513-556-6377

ABSTRACT

$\text{HN}(\text{CH}_2\text{CH}_2\text{PR}_2)_2$ -ligated copper borohydride complexes, $(\text{RPN}^{\text{HP}})\text{Cu}(\text{BH}_4)$ ($\text{R} = i\text{Pr}, \text{Cy}, t\text{Bu}$), which can be prepared from $(\text{RPN}^{\text{HP}})\text{CuBr}$ and NaBH_4 , are capable of catalyzing the hydrogenation of aldehydes in an alcoholic solvent. More active hydrogenation catalysts are $(\text{RPN}^{\text{HP}})\text{CuBr}$ mixed with KO^tBu , allowing various aldehydes and ketones to be efficiently reduced to alcohols except those bearing a nitro, *N*-unprotected pyrrole, pyridine, or an ester group, or those prone to aldol condensation (e.g., 1-heptanal). Modifying the catalyst structure by replacing the NH group in $(i\text{PrPN}^{\text{HP}})\text{CuBr}$ with an NMe group results in an inferior catalyst but preserves some catalytic activity. The hexanuclear copper hydride cluster, $(i\text{PrPN}^{\text{HP}})_3\text{Cu}_6\text{H}_6$, is also competent in catalyzing the hydrogenation of aldehydes such as benzaldehyde and *N*-methyl-2-pyrrolicarboxaldehyde, albeit accompanied by decomposition pathways. The catalytic performance can be enhanced through the addition of a strong base or $i\text{PrPN}^{\text{HP}}$. The three catalytic systems likely share the same catalytically active species, which is proposed to be a mononuclear copper hydride $(\text{RPN}^{\text{HP}})\text{CuH}$ with the NH group bound to copper.

INTRODUCTION

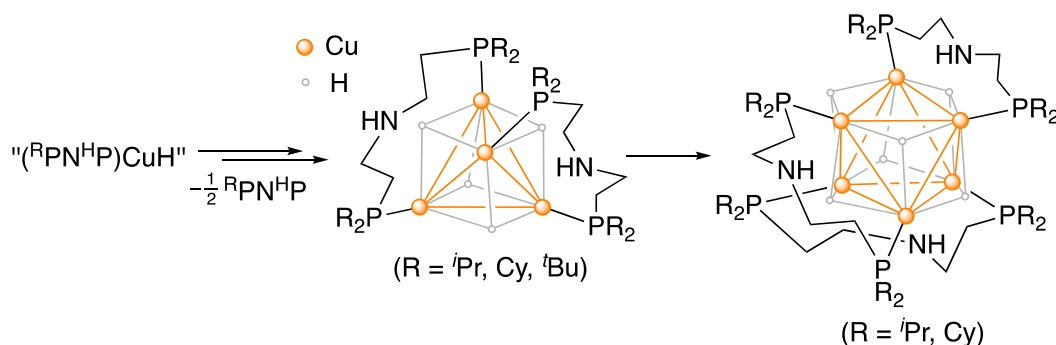
Catalytic reduction of carbonyl compounds has been researched for decades owing to its importance in chemical synthesis, though in recent years efforts have been devoted more to the development of first row metal-based catalysts.¹ Among various reduction strategies, hydrogenation reactions are often preferred when the costs of the reductant and waste disposal outweigh the risks and capital costs for working with a flammable gas. One popular class of pro-ligands used to design catalysts specifically for carbonyl hydrogenation involves a diphosphine of the type $\text{HN}(\text{CH}_2\text{CH}_2\text{PR}_2)_2$ ($^{\text{R}}\text{PN}^{\text{H}}\text{P}$ for short),² which typically binds to metals through the [PNP] donor array. The presence of a metal-bound NH group is thought to play a crucial role in activating the C=O bond and stabilizing high-energy intermediates.^{2,3} While the electronic configuration of the metal ion and the molecular geometry are undoubtedly important for catalysis, metal complexes bearing a ($^{\text{R}}\text{PN}^{\text{H}}\text{P}$)MH (M = Ru, Os, Ir, Re, Mo, Fe, Co, Mn) component² are almost universally successful in catalyzing the hydrogenation of C=O bonds with very few exceptions (e.g., when M = Ni).⁴

Copper-based catalysts for carbonyl hydrogenation have been known since the late 1980s when Stryker's reagent, $(\text{Ph}_3\text{P})_6\text{Cu}_6\text{H}_6$, was studied for the reduction of α,β -unsaturated aldehydes and ketones.⁵ Depending on the hydrogen pressure, 2-cyclohexen-1-one is selectively converted to cyclohexanone ($p_{\text{H}_2} = 65$ psig) or cyclohexanol ($p_{\text{H}_2} > 185$ psig, over an extended period of time). Under the hydrogenation conditions, the catalyst degrades to black particles, which is avoidable through the addition of excess Ph_3P , leading to selective hydrogenation of the C=C–C=O moiety over an isolated C=C bond.^{5b} Catalytic hydrogenation of simple ketones using well-defined copper hydrides such as $(\text{Ph}_3\text{P})_6\text{Cu}_6\text{H}_6$, $(\kappa^2\text{-triphos})_2\text{Cu}_2\text{H}_2$ (triphos = 1,1,1-tris(diphenylphosphinomethyl)ethane), and $(\text{dppp})_4\text{Cu}_8\text{H}_8$ (dppp = 1,3-

bis(diphenylphosphino)propane) proves to be unsuccessful unless the pro-ligand is also added (e.g., $(\text{Ph}_3\text{P})_6\text{Cu}_6\text{H}_6$ with 36 equiv Me_2PPh ; $(\kappa^2\text{-triphos})_2\text{Cu}_2\text{H}_2$ with 1-1.5 equiv triphos).⁶ However, exactly how these added pro-ligands promote the reduction is not well understood. For the hydrogenation of CO_2 to formate,⁷ the cationic copper hydride $[(\kappa^3\text{-triphos})_2\text{Cu}_2\text{H}]^+$ alone is an efficient catalyst.⁸ According to the proposed mechanism, 1,8-diazabicyclo[5.4.0]undec-7-ene (DBU), which is the base needed to drive the reaction, plays another role by breaking the $\text{Cu}(\mu\text{-H})\text{Cu}$ core to yield $[(\kappa^3\text{-triphos})\text{Cu}(\text{DBU})]^+$ and the presumed active species $(\kappa^3\text{-triphos})\text{CuH}$.^{8,9} A very recent study by the Tanase group shows that larger copper clusters, $[(\mu\text{-dpmppm})_3\text{Cu}_8\text{H}_6](\text{PF}_6)_2$ ($\text{dpmppm} = \text{Ph}_2\text{PCH}_2\text{P}(\text{Ph})\text{CH}_2\text{P}(\text{Ph})\text{CH}_2\text{PPh}_2$) and its CO_2 insertion product $[(\mu\text{-dpmppm})_2\text{Cu}_4(\text{OCHO})_3]\text{PF}_6$, are also capable of catalyzing the hydrogenation of CO_2 to HCO_2^- in the presence of DBU.¹⁰

There are also a number of studies involving in-situ generated but structurally ill-defined copper hydrides for catalytic hydrogenation of $\text{C}=\text{O}$ bonds. In particular, copper-catalyzed asymmetric hydrogenation of ketones is often carried out using a chiral phosphine mixed with $\text{Cu}(\text{OAc})_2$, CuCl_2 , or $\text{Cu}(\text{NO}_3)(\text{PAR}_3)_2$.¹¹ These catalytic systems typically require a large excess of strong base (6-25 equiv per copper) and, in some cases,^{11a-d} additional PAR_3 to stabilize the catalysts. A similar catalytic protocol has been applied to chemoselective hydrogenation of aldehydes.¹² Hydrogenation of CO_2 to formate in the presence of DBU or a secondary amine can also be catalyzed by $\text{Cu}(\text{OAc})_2$,¹³ $\text{Cu}(\text{OAc})_2\text{-DMAP}$ ($\text{DMAP} = 4\text{-dimethylaminopyridine}$),¹⁴ or $(\text{dtbpf})\text{CuI}$ ($\text{dtbpf} = 1,1'\text{-bis}(\text{di-}t\text{-butylphosphino})\text{ferrocene}$).¹⁵ Considering that copper hydrides are usually air sensitive,^{7,16} using a simple copper salt such as $\text{Cu}(\text{OAc})_2$ to catalyze the hydrogenation reactions is synthetically more attractive; however, very limited mechanistic details can be gained from these studies.

This work fills several knowledge gaps concerning hydrogenation catalysis with copper. First, although $^{\text{R}}\text{PN}^{\text{H}}\text{P}$ -ligated copper complexes have been known for a decade,¹⁷ they have not been reported as hydrogenation catalysts until now. Our recent study shows that, unlike other metal systems, the putative " $^{\text{R}}\text{PN}^{\text{H}}\text{P}$)CuH" has the tendency to form clusters with only the phosphorus donors bound to copper (along with fully dissociated $^{\text{R}}\text{PN}^{\text{H}}\text{P}$, see Scheme 1).¹⁸ This raises an interesting mechanistic question regarding the role that the NH group may or may not need to play during the hydrogenation process, which is addressed in this work. We have also previously observed the expansion of clusters from $(^{\text{R}}\text{PN}^{\text{H}}\text{P})_2\text{Cu}_4\text{H}_4$ ($\text{R} = ^i\text{Pr}, \text{Cy}$) to $(^{\text{R}}\text{PN}^{\text{H}}\text{P})_3\text{Cu}_6\text{H}_6$ and, in one case ($\text{R} = ^i\text{Pr}$), the release of $(^{\text{R}}\text{PN}^{\text{H}}\text{P})_2\text{Cu}_4\text{H}_4$ when $(^{\text{R}}\text{PN}^{\text{H}}\text{P})_3\text{Cu}_6\text{H}_6$ is treated with PhCHO.¹⁸ Further mechanistic investigation presented herein paves the road for a better understanding of how the formation of copper hydride clusters impacts the overall hydrogenation reactions. Also studied here are the effects of base additives, which have been routinely used in conjunction with copper-based hydrogenation catalysts.



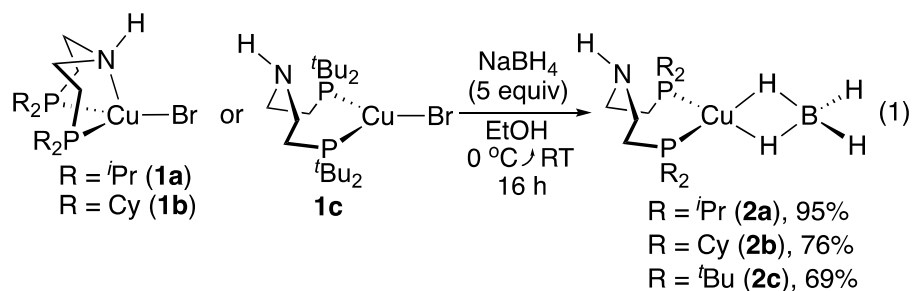
Scheme 1. Aggregation of the putative " $^{\text{R}}\text{PN}^{\text{H}}\text{P}$)CuH"

RESULTS AND DISCUSSION

$(^{\text{R}}\text{PN}^{\text{H}}\text{P})\text{Cu}(\text{BH}_4)$ as Hydrogenation Catalysts. From the outset, we sought a more straightforward method of generating $(^{\text{R}}\text{PN}^{\text{H}}\text{P})\text{CuH}$ in situ to catalyze the hydrogenation of C=O

bonds. Metal borohydride complexes $L_nM(BH_4)$ can be metal hydride complexes L_nMH in disguise, and if needed, a base can be added to assist the removal of BH_3 .¹⁹ For systems in which the hydride species are thermally unstable, it is advantageous to employ the more stable borohydride derivatives as hydrogenation catalysts. Successful examples known to date have been primarily focused on group 8 metal complexes such as *trans*- $RuH(BH_4)(P-P)(1,2\text{-diamine})$ ($P-P$ = a diphosphine or diphosphinite),²⁰ $(^RPN^HP)RuH(CO)(BH_4)$,²¹ $(^RPN^HP)FeHL(BH_4)$ ($L = CO$ or CNR'),²² and $(^iPrPN^MeP)FeH(CNR')(BH_4)$ ($^iPrPN^MeP = MeN(CH_2CH_2P^iPr_2)_2$).²³ For copper-based systems, borohydride complexes are known in the literature,²⁴ although they have not yet been described in hydrogenation studies.

The target copper borohydride complexes bearing a $^RPN^HP$ ligand were readily synthesized by treating $(^RPN^HP)CuBr$ (**1a-c**) with excess $NaBH_4$ (eq 1). The isolated products, which are white solids, can be exposed to air for several hours without noticeable color or spectral change. Under an inert atmosphere, a solution sample of **2a** in C_6D_6 was shown to survive mild heating ($50\text{ }^\circ C$) for at least 2 h but, after 24 h, yield a very small amount of black particles. Nevertheless, its thermal stability is significantly higher than that of the copper hydride complex, $(^iPrPN^HP)_3Cu_6H_6$ (**3a**), which starts to decompose in hours even if kept at room temperature.



2a-c were characterized by NMR and IR spectroscopy as well as elemental analysis. For samples dissolved in C_6D_6 , the BH_4 proton resonances cannot be definitively located due to broadening and overlap with the resonances of the phosphorus substituents (i.e., the R groups).

The ^{11}B NMR spectra, on the other hand, show a distinctive boron resonance near -30 ppm (Table 1), which is resolved as a quintet for **2a** and **2c**. At least one $\text{B-H}_{\text{terminal}}$ and one $\text{B-H}_{\text{bridging}}$ stretching bands can be identified from each IR spectrum (of a solid sample). The frequencies are very similar to those reported for other phosphine-ligated copper borohydride complexes.²⁴ It is interesting to note that the N-H stretching vibration of each copper complex is blue-shifted relative to $^{\text{R}}\text{PN}^{\text{H}}\text{P}$. This result argues against nitrogen coordination, which usually causes a decrease in the N-H stretching frequency.²⁵ The reason for the blue-shift is unclear; the N-H bond contraction can be a result of short-range repulsive forces or electric field effects exerted by the neighboring molecule.²⁶

Table 1. Selected NMR and IR data of **2a-c** and the corresponding pro-ligands

Compound	δ_{B} (ppm)	$\nu_{\text{N-H}}$ (cm^{-1})	$\nu_{\text{B-H}_{\text{terminal}}}$ (cm^{-1})	$\nu_{\text{B-H}_{\text{bridging}}}$ (cm^{-1})
$(^i\text{PrPN}^{\text{H}}\text{P})\text{Cu}(\text{BH}_4)$ (2a)	-29.0 (quint)	3305	2355	2020
$^i\text{PrPN}^{\text{H}}\text{P}$		3285		
$(^{\text{Cy}}\text{PN}^{\text{H}}\text{P})\text{Cu}(\text{BH}_4)$ (2b)	-29.8 (br)	3304	2349, 2338	2022
$^{\text{Cy}}\text{PN}^{\text{H}}\text{P}$		3288		
$(^t\text{BuPN}^{\text{H}}\text{P})\text{Cu}(\text{BH}_4)$ (2c)	-27.6 (quint)	3299	2353	2058
$^t\text{BuPN}^{\text{H}}\text{P}$		3288		

The solid-state structures of **2a** (Figure 1) and **2c** (see Figure S36 in the ESI) studied by X-ray crystallography establish the κ^2 -coordination mode for the BH_4 ligand and the absence of nitrogen coordination. Given that $^i\text{PrPN}^{\text{H}}\text{P}$ in **1a** serves as a tridentate ligand,¹⁷ the Cu-H bond must be stronger than an $\text{N}\rightarrow\text{Cu}$ bond. Additional driving forces for nitrogen dissociation might come from intermolecular electrostatic interactions between the NH and BH_2 groups, as revealed by the crystal packing ($\text{NH}^{\delta+}\cdots\delta^-\text{HB}$ distance: 2.32-2.98 Å).

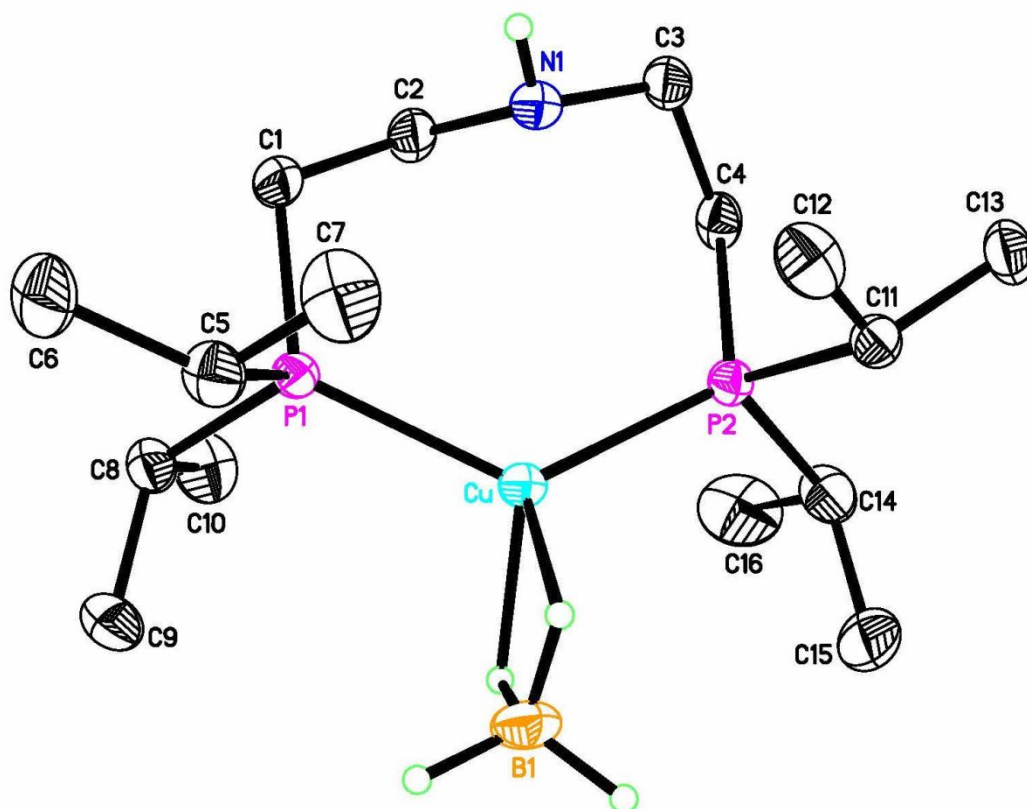
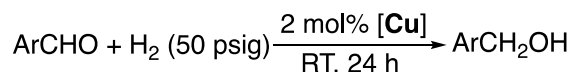
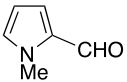
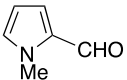


Figure 1. ORTEP drawing of (*i*PrPN^HP)Cu(BH₄) (**2a**) at the 50% probability level (hydrogen atoms bound to nitrogen and boron were located directly from the difference map and their coordinates were refined; all other hydrogen atoms were calculated and treated with a riding model and omitted here for clarity). Selected distances (Å) and angles (deg): Cu–P(1) 2.2605(5), Cu–P(2) 2.2525(5), Cu–B(1) 2.2232(24), Cu...N(1) 3.4471(18); P(1)–Cu–P(2) 127.95(2), B(1)–Cu–P(1) 112.11(7), B(1)–Cu–P(2) 119.52(7), H–Cu–H 65.4(11).

Catalytic activities of **2a-c** (2 mol% loading) for hydrogenation reactions were evaluated at room temperature under 50 psig (or 4.4 bar) H₂ pressure for 24 h. As summarized in Table 2, in THF, all three copper borohydride complexes reduce approximately a stoichiometric amount of PhCHO (entries 1-3). The reduction becomes catalytic when the reaction is carried out in an

alcoholic solvent (entries 4-8). Of the three catalysts tested in *i*PrOH, **2b** is the most active one, resulting in a 99% conversion of PhCHO to PhCH₂OH (entry 7). Under an argon atmosphere using **2a** as the catalyst, 5% of PhCHO is reduced to PhCH₂OH (entry 9), implying that transfer hydrogenation might be operative but would be significantly slower than direct hydrogenation. The addition of KO^tBu in a catalytic amount makes the hydrogenation of PhCHO in THF viable, although the Tishchenko product,²⁷ PhCO₂CH₂Ph, is also produced (entry 10). Reduction of 4-CF₃C₆H₄CHO, which contains a more reactive carbonyl group, can be performed in both THF (entry 11) and *i*PrOH (entry 12). Again, the alcoholic solvent renders the hydrogenation process more efficient. We have previously reported that *N*-methyl-2-pyrrolicarboxaldehyde undergoes insertion into the Cu–H bond of (*i*PrPNHP)₃Cu₆H₆ (**3a**).¹⁸ To our disappointment, this specific aldehyde resists hydrogenation under the catalytic conditions that are effective for PhCHO and 4-CF₃C₆H₄CHO (entry 13). The addition of KO^tBu does not appear to improve the catalytic reaction (entry 14).

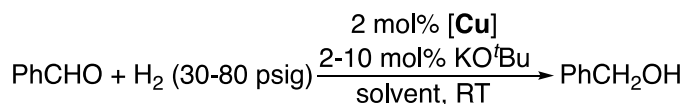
Table 2. Hydrogenation of aldehydes catalyzed by **2a-c**^a

Entry	ArCHO	[Cu]	Solvent	KO ^t Bu (mol%)	Conversion (%) ^b
1	PhCHO	2a	THF	0	1
2	PhCHO	2b	THF	0	2
3	PhCHO	2c	THF	0	2
4	PhCHO	2a	MeOH	0	46
5	PhCHO	2a	EtOH	0	51
6	PhCHO	2a	^t PrOH	0	64
7	PhCHO	2b	^t PrOH	0	99
8	PhCHO	2c	^t PrOH	0	6
9 ^c	PhCHO	2a	^t PrOH	0	5
10	PhCHO	2a	THF	2.4	48(19) ^d
11	4-CF ₃ C ₆ H ₄ CHO	2a	THF	0	7
12	4-CF ₃ C ₆ H ₄ CHO	2a	^t PrOH	0	>99
13		2a	^t PrOH	0	0
14		2a	^t PrOH	2	1

^aStandard conditions: ArCHO (1.0 mmol) and copper catalyst (0.020 mmol) in THF or an alcoholic solvent (3 mL), under H₂ (50 psig), at room temperature (23 °C), stirred for 24 h. ^bDetermined by ¹H NMR spectroscopy. ^cThe reaction was carried out under argon (1 bar) instead of H₂. ^dThe number in the parenthesis is the conversion of PhCHO to PhCO₂CH₂Ph.

NMR studies of **2a** in CD₃OD shed some light on why alcoholic solvents favor the hydrogenation process. The copper borohydride complex proves to be stable in CD₃OD for at least several days, at which point a small amount of HD ($\delta_{\text{H}} = 4.52$ ppm, triplet, $J_{\text{H-D}} = 42.8$ Hz) can be detected. The ¹¹B NMR spectrum shows a quintet at -30.9 ppm for the BH₄ resonance along with a singlet at 3.0 ppm consistent with [B(OCD₃)₄]⁻.²⁸ Thus it is tempting to propose that iterative protonation of the B–H bonds in **2a** by an alcohol will eventually unmask (^tPrPN^HP)CuH to initiate carbonyl reduction. However, these protonation steps are considerably slower than the overall hydrogenation reaction. The BH₄ resonance of **2a** in the ¹H NMR spectrum is observed as a relatively sharp quartet at 0.71 ppm ($J_{\text{H-B}} = 81$ Hz), suggesting increased symmetry around the

illustrated in Scheme 1. Optimizations focusing on room-temperature hydrogenation of PhCHO catalyzed by **1a** and KO^tBu (added in slight excess) show that, in THF, a catalyst loading of 2 mol% and a H₂ pressure of 50 psig are sufficient for the reaction to occur. After 24 h, 98% of PhCHO is reduced to PhCH₂OH while the remaining aldehyde is converted to PhCO₂CH₂Ph (Table 3, entry 1). Changing the catalyst to the cyclohexyl derivative (**1b**) results in a cleaner reduction of PhCHO and shortens the reaction time to 6 h (entry 2). In contrast, using the *tert*-butyl derivative (**1c**) makes the hydrogenation process more sluggish and yields more PhCO₂CH₂Ph (entry 3). The hydrogenation reaction can also be performed in toluene, dioxane, and Et₂O, though less efficiently (entries 4-6). Lowering the H₂ pressure to 30 psig (entry 7) or raising the temperature to 50 °C (entry 8) leads to a precipitous drop in the conversion of PhCHO to PhCH₂OH. The ^RPN^HP ligand is clearly needed; without it, the Tishchenko reaction converting PhCHO to PhCO₂CH₂Ph becomes the more dominant pathway (entry 9). Because KO^tBu³⁰ and metal alkoxides²⁷ are known to catalyze the Tishchenko reaction, their steady-state concentrations should be kept low to minimize the ester formation. Consistent with this hypothesis, reducing the amount of KO^tBu from 2.4 to 2.0 mol% suppresses the formation of PhCO₂CH₂Ph completely (entry 10), whereas adding more KO^tBu increases the percentage of PhCHO being converted to the ester (entry 11). It should be noted that, in the absence of KO^tBu, **1a** alone is not a hydrogenation catalyst (entry 12). Finally, using the optimized **1a**-to-KO^tBu ratio (1 : 1), PhCHO is almost fully reduced to PhCH₂OH in 3 h under 65 psig H₂ pressure (entry 13) or in 1 h under 80 psig H₂ pressure (entry 14).

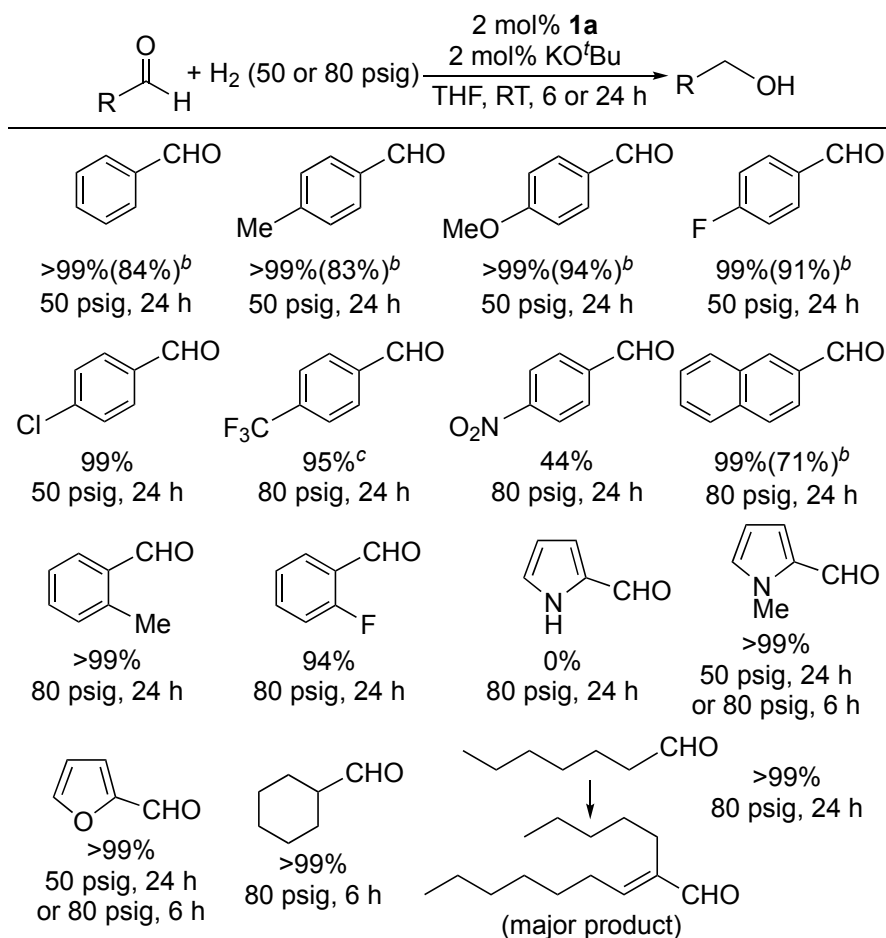
Table 3. Hydrogenation of PhCHO catalyzed by **1a-c** along with KO^tBu^a

Entry	[Cu]	KO ^t Bu (mol%)	Solvent	<i>p</i> _{H₂} (psig)	Time (h)	Conversion (%) ^{b,c}
1	1a	2.4	THF	50	24	98(2)
2	1b	2.4	THF	50	6	>99(0)
3	1c	2.4	THF	50	24	21(10)
4	1a	2.4	toluene	50	24	90(3)
5	1a	2.4	dioxane	50	24	85(2)
6	1a	2.4	Et ₂ O	50	24	15(2)
7	1a	2.4	THF	30	24	8(19)
8 ^d	1a	2.4	THF	50	24	6(10)
9	CuBr	2.4	THF	50	6	5(21)
10	1a	2.0	THF	50	24	>99(0)
11	1a	10	THF	50	24	66(28)
12	1a	0	THF	50	6	0(0)
13	1a	2.0	THF	65	3	99(0)
14	1a	2.0	THF	80	1	98(0)

^aStandard conditions: PhCHO (1.0 mmol), copper complex (0.020 mmol), and KO^tBu in a solvent (3 mL), under H₂, stirred at room temperature (23 °C). ^bDetermined by ¹H NMR spectroscopy. ^cNumbers in the parentheses are the conversions of PhCHO to PhCH₂OH. ^dStirred at 50 °C.

The substrate scope of the copper-catalyzed hydrogenation reactions was explored by employing **1a**-KO^tBu as the catalyst (2 mol% loading). The results for aldehydes are summarized in Table 4. Under the conditions optimized for PhCHO (*p*_{H₂} = 50 psig, room temperature, 24 h), benzaldehyde derivatives bearing an electron-donating or a weakly electron-withdrawing group at the *para* position are hydrogenated nearly quantitatively to yield the corresponding alcohols. In our recent study of the reactions between {2,6-(*i*-Pr₂PO)₂C₆H₃}NiH and aldehydes,³¹ 4-CF₃C₆H₄CHO was shown to perform consecutive insertions more readily than PhCHO which, following a β-hydride elimination step, gave the Tishchenko product. In line with this finding, hydrogenation of 4-CF₃C₆H₄CHO catalyzed by **1a**-KO^tBu is plagued by the competing ester-forming process. A selectivity of 95% for 4-CF₃C₆H₄CH₂OH can be achieved when the H₂

pressure is increased to 80 psig and the reaction mixture is diluted by twofold. Hydrogenation of 4-NO₂C₆H₄CHO is incomplete after 24 h even under 80 psig H₂ pressure (44% conversion), likely due to oxidation of the copper hydride intermediate by the nitro group. 2-Naphthaldehyde, 2-CH₃C₆H₄CHO, and 2-FC₆H₄CHO react more slowly than PhCHO and their *para*-isomers, thus requiring a slightly higher H₂ pressure (80 psig). Pyrrole-2-carboxaldehyde is not a viable substrate for the catalytic system. The NH moiety must prevent dihydrogen activation by strongly interacting with copper, which is indirectly confirmed by successful hydrogenation of *N*-methyl-2-pyrrolecarboxaldehyde and furfural. Hydrogenation of aliphatic aldehydes is feasible, as successfully demonstrated with cyclohexanecarboxaldehyde. 1-Heptanal, on the other hand, mainly participates in aldol condensation reaction, forming (*E*)-2-pentyl-2-nonenal³² as the major product.

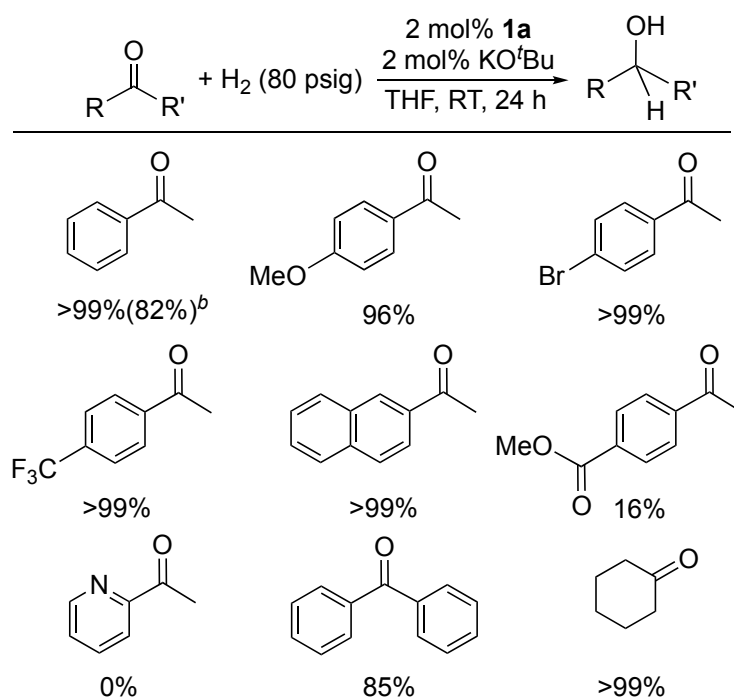
Table 4. Hydrogenation of various aldehydes catalyzed by **1a** along with KO^tBu^a

^aStandard conditions: RCHO (1.0 mmol), **1a** (0.020 mmol), and KO^tBu (0.020 mmol) in THF (3 mL), under H₂ (50 or 80 psig), stirred at room temperature (23 °C); conversions were determined by ¹H NMR spectroscopy. ^bNumbers in the parentheses are isolated yields. ^cThe volume of THF was increased to 6 mL; 5% of RCHO was converted to RCO₂CH₂R.

Hydrogenation of ketones catalyzed by **1a**-KO^tBu (2 mol% loading) was performed under 80 psig H₂ pressure. As shown in Table 5, a quantitative conversion of acetophenone to 1-phenylethanol can be accomplished in 24 h. Under the same conditions, acetophenone derivatives substituted by a methoxy, bromo, or trifluoromethyl group at the *para* position or fused by a benzene ring (e.g., 2-acetylnaphthalene) are hydrogenated smoothly to the corresponding alcohols.

Hydrogenation of methyl 4-acetylbenzoate occurs selectively to the ketone functionality but with a surprisingly low conversion of 16%. A more problematic substrate is 2-acetylpyridine, which may deactivate the catalyst through nitrogen coordination. As representative examples for diaryl ketones and aliphatic ketones, benzophenone and cyclohexanone are reduced to diphenylmethanol and cyclohexanol, respectively, without any issues.

Table 5. Hydrogenation of various ketones catalyzed by **1a** along with KO^tBu^a

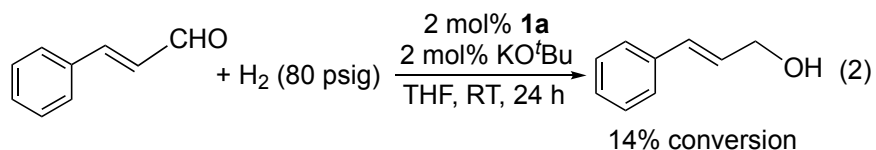


^aStandard conditions: RCOR' (1.0 mmol), **1a** (0.020 mmol), and KO^tBu (0.020 mmol) in THF (3 mL), under H₂ (80 psig), stirred at room temperature (23 °C); conversions were determined by ¹H NMR spectroscopy. ^bThe number in the parenthesis is the isolated yield.

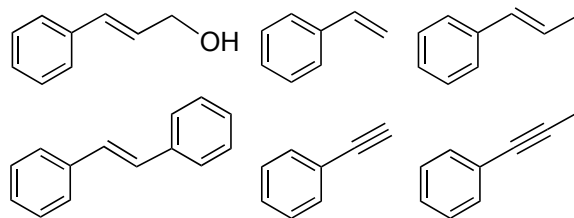
Given that aldehydes can be hydrogenated under a lower H₂ pressure than that for ketones (50 vs. 80 psig), an attempt was made to selectively reduce the aldehyde functionality of 4-acetylbenzaldehyde using the conditions optimized for benzaldehyde (Table 3, entry 10).

Unfortunately, the reaction did not yield any alcohol product; instead, a highly insoluble material was obtained upon mixing the substrate with the catalyst. It is possible that 4-acetylbenzaldehyde oligomerized or polymerized via an iterative aldol reaction.

To probe the selectivity in the hydrogenation of α,β -unsaturated aldehydes and ketones, 2-cyclohexen-1-one, 4-phenyl-3-buten-2-one, and cinnamaldehyde were treated with 2 mol% **1a**-KO^tBu (in THF) under 80 psig H₂ pressure. For reasons unclear to us, the two ketone substrates gave rise to a complicated mixture that was difficult to analyze.³³ In contrast, hydrogenation of cinnamaldehyde formed cinnamyl alcohol only, albeit with a low conversion (eq 2). The same chemoselectivity (C=O over C=C bond) has been observed in two other copper-based catalytic systems: (1) (Ph₃P)₆Cu₆H₆ (5 mol% Cu), Me₂PPh (6 equiv/Cu), ^tBuOH (40 equiv/Cu), in C₆H₆, 55 psig H₂, RT;^{6a} (2) Cu(NO₃)(PPh₃)₂-Ph₂P(CH₂)₄PPh₂ (0.2 mol%), NaOH (10 equiv/Cu), in EtOH, 710 psig H₂, 50 °C.¹²

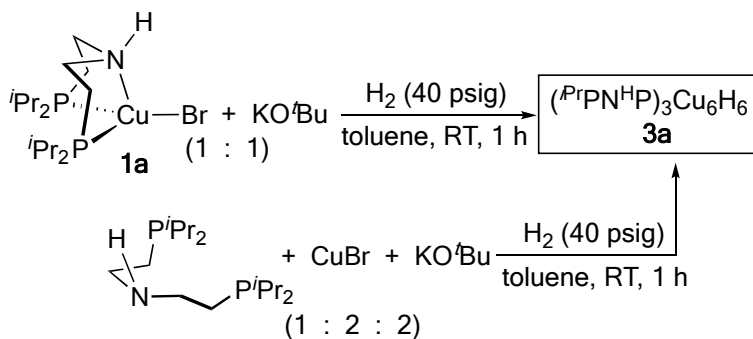


The aforementioned result indicates that the C=C bond in cinnamyl alcohol resists hydrogenation, which was confirmed separately by using pure cinnamyl alcohol as the substrate. Under the same conditions outlined in eq 2, styrene, *trans*- β -methylstyrene, *trans*-stilbene, phenylacetylene, and 1-phenyl-1-propyne are completely unreactive (Scheme 3). Diphenylacetylene, however, shows some reactivity, giving *cis*-stilbene (4%) and *trans*-stilbene (5%) as determined by GC-MS and NMR.



Scheme 3. Substrates resistant to hydrogenation

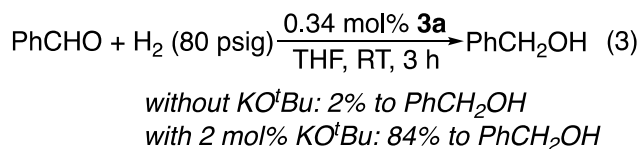
$(iPrPN^H P)_3Cu_6H_6$ as a Hydrogenation Catalyst. Without a reducible substrate, the reaction of **1a** with KO^tBu under H₂ (Scheme 4) would generate $(iPrPN^H P)_3Cu_6H_6$ (**3a**) along with $iPrPN^H P$.¹⁸ A smaller aggregate $(iPrPN^H P)_2Cu_4H_4$ is also observable as the transient intermediate. The hexanuclear cluster can alternatively be prepared from $iPrPN^H P$, CuBr, and KO^tBu using the ligand-to-copper ratio suggested by the formula (1 : 2). Regardless of the routes used, the rates at which these clusters are formed (requiring 30-60 min) are comparable to the catalytic turnover frequencies (2-8 h⁻¹), suggesting that the cluster formation could be kinetically relevant for the hydrogenation process.



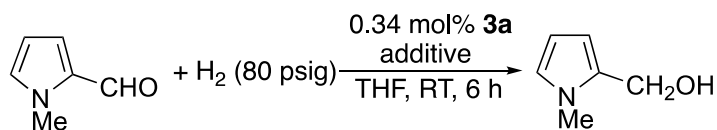
Scheme 4. Synthetic routes to the copper hydride cluster **3a**

To further understand the catalytic roles that the hydride clusters might play, pure **3a** was employed as a hydrogenation catalyst. Because each molecule of **3a** contains six copper atoms, the catalyst loading was reduced to 0.34 mol% so that the total copper loading remained at 2 mol%. Hydrogenation of PhCHO (1 mmol in 3 mL of THF), as demonstrated in eq 3, proves to be very

slow, providing an essentially stoichiometric amount of PhCH₂OH. Interestingly, adding a catalytic amount of KO^tBu accelerates the hydrogenation of PhCHO to PhCH₂OH. As expected, the presence of KO^tBu also diverts 16% of PhCHO to PhCO₂CH₂Ph.



Compared to PhCHO, *N*-methyl-2-pyrrolecarboxaldehyde is less prone to forming the Tishchenko product. Its hydrogenation catalyzed by **3a** produces *N*-methyl-2-(hydroxymethyl)pyrrole exclusively, even when KO^tBu is added (Table 6). Under the catalytic conditions that **1a**-KO^tBu would reduce this aldehyde fully to the alcohol, **3a** is catalytically active but results in an incomplete reaction (entry 1). Similar to the outcomes shown in eq 3, the addition of KO^tBu or a related strong base such as LiO^tBu and NaN(SiMe₃)₂ speeds up the hydrogenation process (entries 2-5). Screening of weak bases reveals that Et₃N increases the hydrogenation rate slightly (entry 6), whereas *N,N*-diisopropylethylamine and 2,6-lutidine slow down the reaction (entries 7 and 8). Phosphine oxides are known to stabilize Cu(I) and Cu(II) species,³⁴ and ^tBuOH is sometimes added to stabilize Cu(I) alkoxide intermediates (through alkoxide exchange to form the more stable L_nCuO^tBu).^{6a} Our results show that neither additive has any effect on the hydrogenation reaction (entries 9 and 10).

Table 6. Hydrogenation of *N*-methyl-2-pyrrolicarboxaldehyde catalyzed by **3a**^a

Entry	Additive	Conversion (%) ^b
1	none	63
2	KO ^t Bu (2 mol%)	94
3	KO ^t Bu (4 mol%)	95
4	LiO ^t Bu (2 mol%)	91
5	NaN(SiMe ₃) ₂ (2 mol%)	96
6	Et ₃ N (2 mol%)	76
7	<i>N,N</i> -diisopropylethylamine (2 mol%)	34
8	2,6-lutidine (2 mol%)	41
9	Ph ₃ P=O (2 mol%)	61
10	^t BuOH (2 mol%)	59
11	ⁱ PrPN ^H P (1 mol%)	99

^aStandard conditions: *N*-methyl-2-pyrrolicarboxaldehyde (1.0 mmol), **3a** (0.0034 mmol, 2 mol% Cu), and an additive in THF (3 mL), under H₂ (80 psig), stirred at room temperature (23 °C).

^bDetermined by ¹H NMR spectroscopy.

It is worth noting again that **3a** and the smaller aggregate (ⁱPrPN^HP)₂Cu₄H₄ have a ligand-to-copper ratio of 1 : 2 (Scheme 1). If the integrality of these clusters were maintained during the hydrogenation reaction, adding ⁱPrPN^HP to the catalytic mixture could potentially interfere with the approach of the substrate and H₂ to copper. However, if the clusters needed to be broken down into (ⁱPrPN^HP)_nCu_nH_n (n = 1-3)³⁵ for the hydrogenation reaction to occur, added ⁱPrPN^HP could be beneficial because in theory 50% of the CuH moieties would be unsupported and decompose to Cu(0) and H₂.³⁶ Consistent with the latter, adding 1 mol% ⁱPrPN^HP leads to a marked improvement of the hydrogenation reaction (entry 11).

The NH Effect. Hydrogenation catalysts bearing a (^RPN^HP)MH component often operate via a metal-ligand bifunctional mechanism in which the NH functionality activates the carbonyl

substrates, stabilizes the intermediates following hydride transfer, and participates in dihydrogen activation, all enabled by the N–H···O hydrogen-bonding interactions (HBIs).³ When the NH group is alkylated, these benefits disappear and the hydride becomes sterically less accessible, leading to inactive catalysts. The presence of an H–N–M–H unit, however, does not necessarily mean that the NH group is always involved in the hydrogenation mechanism. The H–N–M–H dihedral angle can be too wide (e.g., 60° or higher) to participate in N–H···O HBIs that are conformationally restricted by the metal.³⁷ Furthermore, in some catalytic systems (e.g., iron-catalyzed hydrogenation of CO₂), the N–H···O HBIs can be unimportant.^{23,38} Alkylating the NH group in these catalysts makes little difference on the catalytic performance, or even shows improvement, possibly due to increased thermal stability for the *N*-alkylated catalysts.³⁷ The copper system presented in this work is unique in the sense that the NH binding is not guaranteed, which depends on the nature of the X-type ligand on Cu(I). For instance, nitrogen coordination is absent in (RPN^HP)Cu(BH₄), (RPN^HP)₂Cu₄H₄, and (RPN^HP)₃Cu₆H₆, but present in (RPN^HP)CuBr unless the phosphorus substituents are sufficiently bulky (R = ^tBu, see structure of **1c** in eq 1). If the catalytically active species lack nitrogen coordination, alkylating the NH group is expected to have a minimal impact on the catalytic activity.³⁹

Guided by this analysis, we prepared the *N*-methylated copper complex, (ⁱPrPN^{Me}P)CuBr (**4a**), from ⁱPrPN^{Me}P and CuBr in THF (eq 4) and studied its structure by X-ray crystallography. As illustrated in Figure 2, **4a** is a four-coordinate metal complex with the NMe group bound to copper. The geometry about copper is best described as trigonal pyramidal based on the geometry index (τ_4)⁴⁰ value of 0.83. The Me–N–Cu–Br dihedral angle of 19.68° is comparable to the H–N–Cu–Br dihedral angle in **1a** (24.89° and 25.62° for two independent molecules).¹⁷ If the hypothesized hydride species (ⁱPrPN^HP)_nCu_nH_n (n = 1-3), especially the mononuclear one, do

contain the H–N–Cu–H bond connectivity, the dihedral angle is likely similar, although at this point it is unclear if such angle ($\sim 20^\circ$) remains reasonable for a metal-ligand bifunctional catalyst.

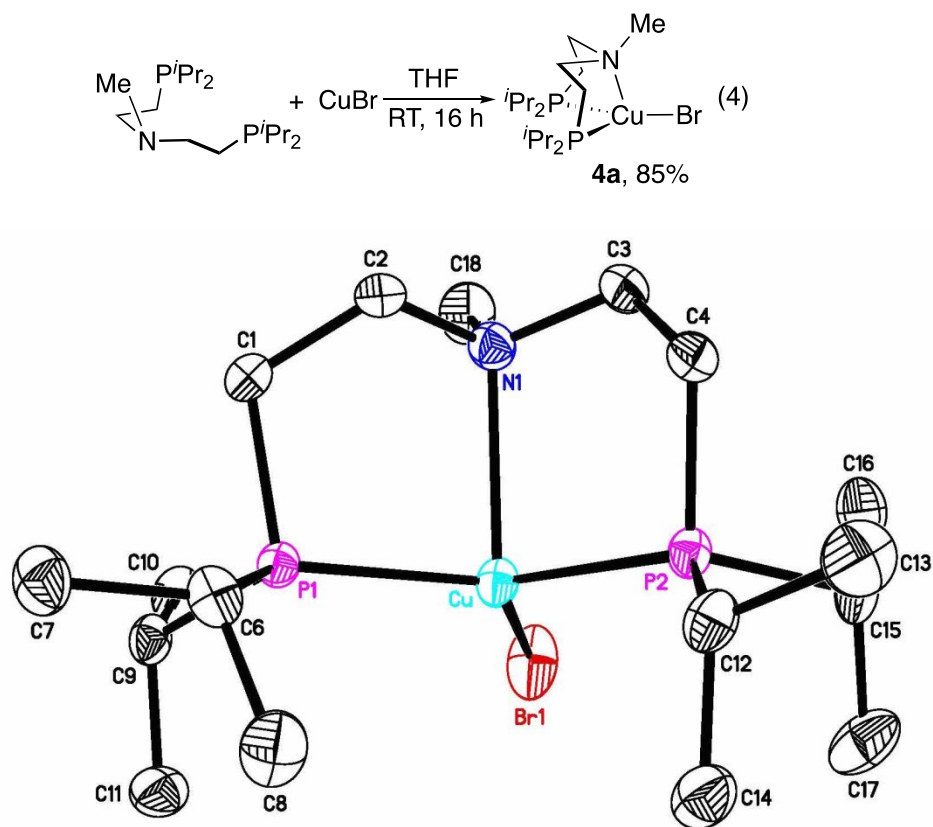
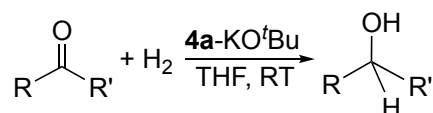


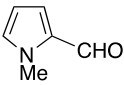
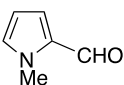
Figure 2. ORTEP drawing of (*i*PrPN^{Me}P)CuBr (**4a**) at the 50% probability level (all hydrogen atoms omitted for clarity). Selected distances (Å) and angles (deg): Cu–P(1) 2.2400(6), Cu–P(2) 2.2363(6), Cu–Br(1) 2.4118(4), Cu–N(1) 2.3654(19); P(1)–Cu–P(2) 125.39(2), N(1)–Cu–P(1) 85.11(5), N(1)–Cu–P(2) 85.41(5), N(1)–Cu–Br(1) 108.87(5), P(1)–Cu–Br(1) 117.740(19), P(2)–Cu–Br(1) 116.228(19).

Catalytic performance of **4a**-KO^tBu was investigated for the hydrogenation of PhCHO, *N*-methyl-2-pyrrolicarboxaldehyde, and PhCOCH₃ (Table 7). Under the conditions that **1a**-KO^tBu would induce high conversions of the carbonyl substrates to the desired alcohols, **4a**-KO^tBu

displays very limited activity (entries 1-3). For the reduction of the two aldehydes, increasing the catalyst loading by fivefold leads to a significant increase in alcohol formation and, in the case of PhCHO, also ester formation (entries 4 and 5). The amounts of alcohol products being formed suggest that these reactions are catalytic in copper and having an NH group is not absolutely required for the catalysts to be active. Nevertheless, the ^RPN^HP-ligated copper complex is substantially more reactive, suggesting that nitrogen coordination is most likely present in the catalytically active species.

Table 7. Hydrogenation of C=O bonds catalyzed by **4a** along with KO^tBu^a



Entry	RCOR'	4a (mol%)	KO ^t Bu (mol%)	<i>p</i> _{H2} (psig)	Time (h)	Conversion (%) ^{b,c}
1	PhCHO	2	2.4	50	24	1(0.4)
2		2	2	80	6	3
3	PhCOCH ₃	2	2.4	80	24	0
4	PhCHO	10	12	50	24	54(43)
5		10	10	80	6	45

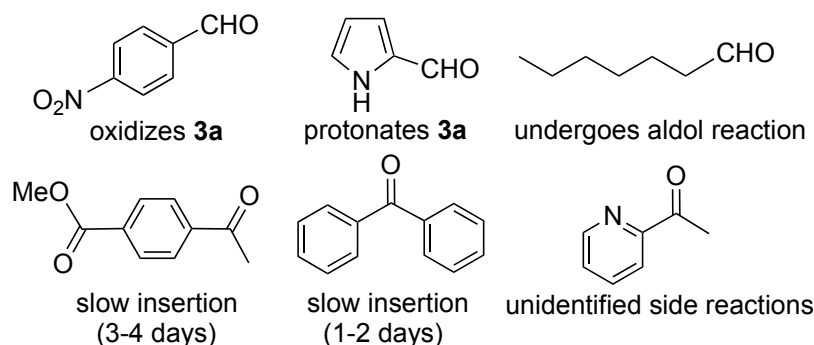
^aStandard conditions: RCOR' (1.0 mmol), **4a**, and KO^tBu in THF (3 mL), under H₂ (50 or 80 psig), at room temperature (23 °C), stirred for 6 or 24 h. ^bDetermined by ¹H NMR spectroscopy. ^cNumbers in the parentheses are the conversions of PhCHO to PhCO₂CH₂Ph.

Mechanistic Considerations. Among the three types of hydrogenation catalysts examined thus far, (^RPN^HP)CuBr mixed with KO^tBu appears to be the most efficient one. It is possible that the copper bromide complexes react with KO^tBu to yield (^RPN^HP)CuO^tBu and/or T-shaped (^RPNP)Cu (with concomitant elimination of HO^tBu),⁴¹ which then activate H₂ to form copper hydrides. Indeed, the colorless solution of **1a** in C₆D₆ turns lemon yellow upon mixing with KO^tBu (1 equiv), indicating some reaction between these two compounds. ¹H and ³¹P{¹H}

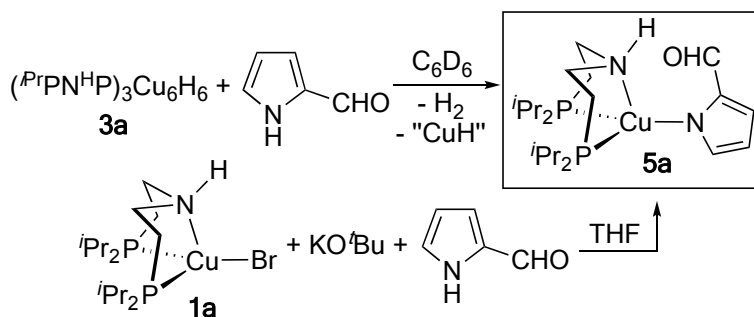
cyclohexanone.^{5b} This result should explain why $(\text{Ph}_3\text{P})_6\text{Cu}_6\text{H}_6$ is a poor hydrogenation catalyst for simple ketones. In studying hydrosilylation mechanisms, Nikonov reported the insertion reaction of PhCHO with $(\text{Ph}_3\text{P})_6\text{Cu}_6\text{H}_6$ which, after a day, gives $(\text{Ph}_3\text{P})_n\text{CuOCH}_2\text{Ph}$ (65% NMR yield) as well as some metallic copper.⁴³ A recent study by Tran and Bullock focusing on $(\text{NHC})_2\text{Cu}_2\text{H}_2$ (NHC = an *N*-heterocyclic carbene) confirms that the dinuclear hydride needs to dissociate to $(\text{NHC})\text{CuH}$ first, and the subsequent reaction with an aldehyde or a ketone produces a copper alkoxide complex.⁴⁴ As also demonstrated by Leysens, Riant, and Sollogoub, a monomeric $(\text{NHC})\text{CuH}$ built inside a cyclodextrin reduces the carbonyl group of acetophenone and 4-phenyl-3-buten-2-one to yield an insertion product.⁴⁵ In our preliminary study, we have shown stoichiometric reduction of PhCHO, *N*-methyl-2-pyrrolicarboxaldehyde, and PhCOCH₃ by **3a** to give copper alkoxide species as the major products.¹⁸ However, the complexity of the NMR spectra does not allow us to identify other products that are potentially generated from these reactions (e.g., $(^R\text{PNP})\text{Cu}$ and $(^R\text{PN}^H\text{P})\text{CuOH}$ resulting from hydrolysis of the alkoxide species).

For this work, we studied the reactivity of **3a** with additional substrates, especially the challenging ones for the catalytic reactions (Scheme 6). In a typical experiment, **3a** was mixed with a carbonyl substrate (10 equiv, or 1.7 equiv on a per CuH basis) in C₆D₆ and the progress of the reaction was monitored by NMR spectroscopy. A successful insertion reaction with **3a** is usually signaled by a color change from orange to brownish yellow. Interestingly, adding 4-nitrobenzaldehyde to **3a** induces an immediate color change to dark green and then to black/brown in 30 min, consistent with a series of oxidation events by the nitro group. The reaction of pyrrole-2-carboxaldehyde with **3a** generates H₂ and **5a**,⁴⁶ which can be synthesized independently from **1a**, KO^tBu, and pyrrole-2-carboxaldehyde (Scheme 7). This confirms our earlier hypothesis that the failure to hydrogenate this specific aldehyde is due to strong substrate binding. 1-Heptanal reacts

with **3a** differently, giving (*E*)-2-pentyl-2-nonenal as the major organic product. The copper alkoxide species resulting from carbonyl insertion must act as a catalyst for the aldol condensation reaction. Methyl 4-acetylbenzoate and benzophenone undergo slow insertion, requiring days to fully consume **3a**. By comparison, the reaction of PhCOCH₃ with **3a** takes 2 h to complete. The reaction with 2-acetylpyridine is very complicated; in addition to the expected insertion product, several other unidentified by-products are also present. Overall, the outcomes of the stoichiometric reactions with **3a** more or less reflect how these carbonyl substrates are reduced catalytically by **1a**-KO^tBu.⁴⁷



Scheme 6. Substrates that lead to low or no conversions to the alcohols



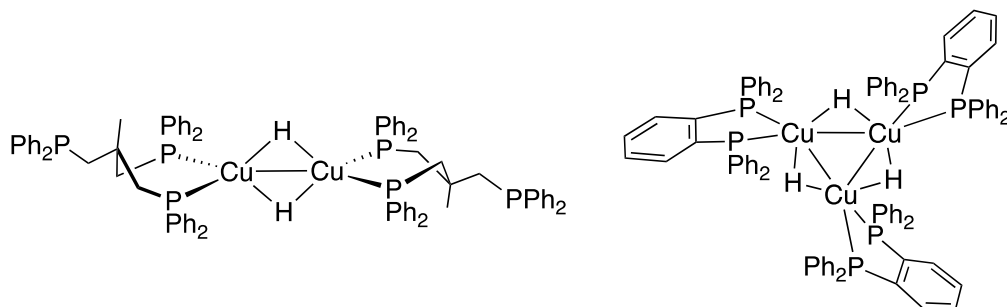
Scheme 7. Copper pyrrolide complex derived from pyrrole-2-carboxaldehyde

The carbonyl insertion into the Cu–H bond of **3a** is an irreversible process, as established by no protio incorporation into the remaining PhCDO during the reaction of **3a** with 10 equiv of PhCDO. Attempts to isolate the insertion products (i.e., the copper alkoxide complexes) including

the independent synthesis from **1a** and NaOCH₂Ph have been fruitless. According to the study by Whitesides,⁴⁸ primary and secondary alkoxide complexes of Cu(I) can undergo facile thermal decomposition via radical intermediates. The added complication to the reaction of **3a** with a carbonyl substrate is that the insertion reaction is always accompanied by the decomposition of **3a**, in part due to the insufficient amount of the supporting ligand. The fact that KO^tBu can enhance the catalytic reactivity of **3a** (eq 3 and Table 6) encouraged us to study the stoichiometric reduction in the presence of added KO^tBu. First, a control experiment confirms that KO^tBu does not react with **3a**. Mixing *N*-methyl-2-pyrrolicarboxaldehyde with **3a** and KO^tBu in a 10 : 1 : 1.2 ratio (in C₆D₆) generates the insertion product more cleanly than the reaction without KO^tBu. In other words, the addition of KO^tBu minimizes the degradation of **3a** during carbonyl insertion, possibly through the increase of negative charge on copper. Adding ^{*i*}PrPN^HP to the reaction of **3a** with *N*-methyl-2-pyrrolicarboxaldehyde can provide the similar benefit.

Taken together, we speculate that the catalytically active species is a mononuclear copper hydride (^RPN^HP)CuH with ^RPN^HP acting as a tridentate ligand. The hexanuclear clusters (^RPN^HP)₃Cu₆H₆ have an intense color (R = ^{*i*}Pr, bright orange; R = Cy, dark red), in contrast to the light yellow color typically observed for a productive hydrogenation reaction. We have also previously isolated tetranuclear clusters (^RPN^HP)₂Cu₄H₄ (R = Cy, ^{*t*}Bu) as off-white solids,¹⁸ so the color alone cannot be used to rule out the involvement of aggregates. Furthermore, even species spectroscopically observable during the catalytic reaction may not be directly involved in the catalytic cycle. It should be pointed out, though, that the NH group does not coordinate to copper in (^RPN^HP)₃Cu₆H₆ and (^RPN^HP)₂Cu₄H₄. We have not yet had spectroscopic evidence for (^RPN^HP)_{*n*}Cu_{*n*}H_{*n*} (*n* = 2, 3); however, based on reported structures of phosphine-ligated dinuclear^{35a} and trinuclear^{35c} copper hydrides (Scheme 8), the NH coordination is unlikely to be involved.

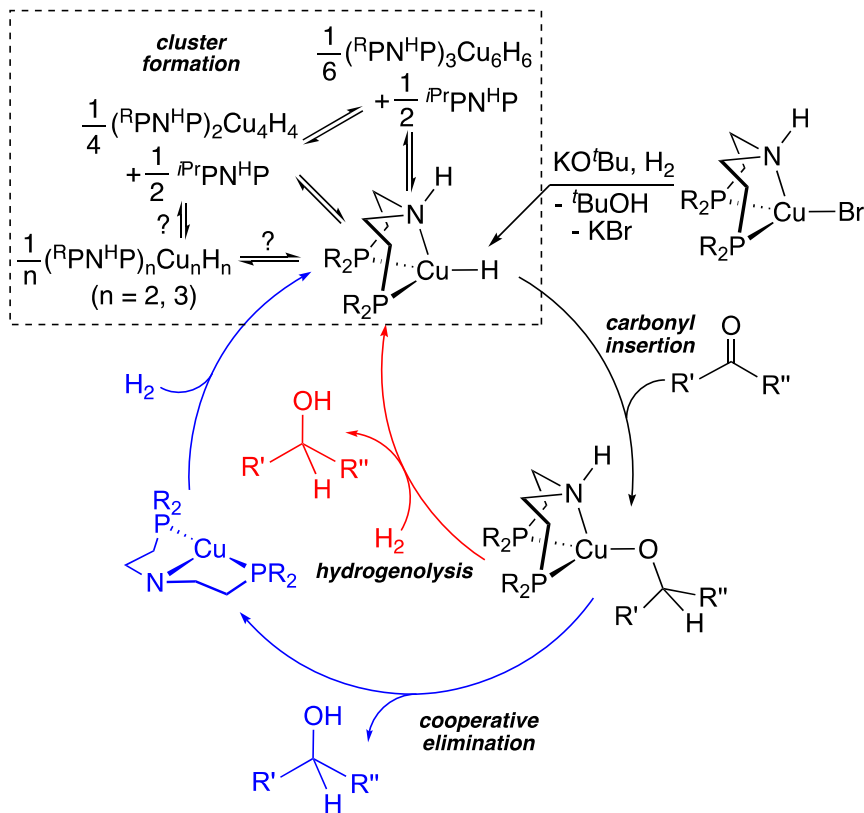
Therefore, we would have anticipated similar catalytic activity exhibited by **1a**-KO^tBu and **4a**-KO^tBu. A significant NH effect, as observed experimentally, is expected for the mononuclear copper hydride (^RPN^HP)CuH where the NH coordination is most likely present.⁴⁹



Scheme 8. Structures of phosphine-ligated dinuclear and trinuclear copper hydrides

Mechanistic pathways consistent with our experimental results are outlined in Scheme 9. Starting from (^RPN^HP)CuBr, its reaction with KO^tBu under H₂ may generate the mononuclear copper hydride (^RPN^HP)CuH, which can aggregate to clusters under the following circumstances: (1) when the substrate is not added, (2) when the substrate is depleted at the end of hydrogenation, and (3) when the substrate reacts with (^RPN^HP)CuH slowly. The productive catalytic cycle begins with carbonyl insertion to form an alkoxide intermediate, which undergoes direct hydrogenolysis to regenerate (^RPN^HP)CuH while releasing the alcohol product. The hydrogenolysis step may require a prior dissociation of the NH group from copper. An alternative or perhaps parallel pathway relies on the NH hydrogen to eliminate the alcohol product from the alkoxide intermediate. The resulting T-shaped copper complex (^RPNP)Cu activates H₂ to close the catalytic cycle.⁵⁰ The observed H₂ pressure dependence (Table 3) and KIE (Scheme 2) imply that dihydrogen activation is the turnover-limiting step, at least for the hydrogenation of PhCHO. The turnover-limiting step could change to the insertion step when a less reactive carbonyl substrate is

used. Alkylating the NH group shuts the cooperative elimination path from the alkoxide intermediate but still allows the hydrogenolysis to occur, which accounts for the observed catalytic activity with $(^R\text{PN}^{\text{Me}}\text{P})\text{CuBr}$. The diminished activity could be due to the unfavorable steric effects on the insertion and hydrogenolysis steps and/or only one hydride-regeneration pathway being available. When the cluster $(^R\text{PN}^{\text{HP}})_3\text{Cu}_6\text{H}_6$ is employed as the catalyst, it can dissociate to $(^R\text{PN}^{\text{HP}})\text{CuH}$, thus entering the catalytic cycle. We cannot, however, rule out an insertion event on the cluster prior to cluster dissociation. Neither can we completely rule out the involvement of $(^R\text{PN}^{\text{HP}})_n\text{Cu}_n\text{H}_n$ ($n = 2, 3$). In a simplistic view, $(^R\text{PN}^{\text{HP}})_3\text{Cu}_6\text{H}_6$ should display 50% of the catalytic activity observed for $(^R\text{PN}^{\text{HP}})\text{CuBr}$ (on a per Cu basis), assuming that half of the copper sites are lost to the short-lived "CuH". In reality, other decomposition reactions also take place from $(^R\text{PN}^{\text{HP}})_3\text{Cu}_6\text{H}_6$ and the extent of decomposition depends on the substrate used. For instance, the reduction of PhCHO with **3a** gives significantly more by-products than the reduction of *N*-methyl-2-pyrrolicarboxaldehyde, which can be used to rationalize the very low PhCHO-to-PhCH₂OH conversions shown in eq 3 (without KO^tBu). In any case, the addition of KO^tBu or $^R\text{PN}^{\text{HP}}$ can minimize the degradation processes, leading to improved catalytic reactions.



Scheme 9. Proposed hydrogenation mechanism

CONCLUSIONS

In this work, we have shown catalytic hydrogenation of C=O bonds with three different types of copper complexes, all bearing a RPNHP ligand: $(\text{RPNHP})\text{Cu}(\text{BH}_4)$ ($\text{R} = i\text{Pr}, \text{Cy}$), $(\text{RPNHP})\text{CuBr}-\text{KO}^t\text{Bu}$ ($\text{R} = i\text{Pr}, \text{Cy}, ^t\text{Bu}$), and $(i\text{PrPNHP})_3\text{Cu}_6\text{H}_6$. The copper borohydride complexes exhibit the lowest catalytic activities. The reactions are best carried out in an alcoholic solvent, which assists the dissociation of BH_4^- from copper to initiate the reduction of aldehydes, first with BH_4^- and then with H_2 . The copper bromide complexes, when combined with KO^tBu , show the highest catalytic activities, allowing a variety of aldehydes and ketones to be hydrogenated to alcohols. Challenging substrates include 4-nitrobenzaldehyde, pyrrole-2-carboxaldehyde, 1-heptanal, and 2-acetylpyridine, and their intended hydrogenation reactions are impeded by other

processes including oxidation or protonation of the hydride intermediates, aldol condensation, and strong binding to copper. Less polar double bonds such as those in styrene and phenylacetylene derivatives are resistant to the hydrogenation conditions. Replacing the NH group in $(i\text{PrPN}^{\text{HP}})\text{CuBr}$ with an NMe group does not lead to a completely inactive catalyst, but the catalytic efficiency is significantly reduced. The hexanuclear copper hydride complex $(i\text{PrPN}^{\text{HP}})_3\text{Cu}_6\text{H}_6$ proves to be an active catalyst for aldehyde hydrogenation. It performs better than $(i\text{PrPN}^{\text{HP}})\text{Cu}(\text{BH}_4)$ but worse than $(i\text{PrPN}^{\text{HP}})\text{CuBr}\text{-KO}^t\text{Bu}$ for the hydrogenation of *N*-methyl-2-pyrrolicarboxaldehyde. The catalytic reactions can be improved through the addition of a strong base or $i\text{PrPN}^{\text{HP}}$.

Copper hydrides are inclined to aggregation to form clusters. For the RPN^{HP} -ligated system, they are known to yield the spectroscopically observable $(\text{RPN}^{\text{HP}})_2\text{Cu}_4\text{H}_4$ ($\text{R} = i\text{Pr}, \text{Cy}, ^t\text{Bu}$) and $(\text{RPN}^{\text{HP}})_3\text{Cu}_6\text{H}_6$ ($\text{R} = i\text{Pr}, \text{Cy}$), in which the central NH group does not coordinate to copper. The cluster-forming process is not slow enough to be completely irrelevant for the catalytic hydrogenation reactions. Though we favor a mononuclear copper hydride $(\text{RPN}^{\text{HP}})\text{CuH}$ with the NH group bound to copper, the catalytically active species could also be a copper hydride cluster. We suspect that the aggregation process can become favorable when the substrates are less reactive towards $(\text{RPN}^{\text{HP}})\text{CuH}$.⁵¹

The effects of base additives have been examined for all three catalytic systems. In THF, with added KO^tBu , the copper borohydride complexes show higher catalytic activities, likely due to the removal of BH_3 to unmask the hydrides. The copper bromide complexes require 1 equiv of KO^tBu to fully activate the catalysts. An excess of KO^tBu can be detrimental to the hydrogenation of aldehydes due to the base-catalyzed Tishchenko reaction. The hexanuclear copper hydride

$(i\text{PrPN}^{\text{HP}})_3\text{Cu}_6\text{H}_6$ displays an improved catalytic efficiency in the presence of KO^tBu, which is shown to minimize the unproductive degradation of the cluster.

EXPERIMENTAL SECTION

General Considerations. All copper complexes described in this paper were prepared under an argon atmosphere using standard glovebox and Schlenk techniques. Benzene- d_6 (purchased from Cambridge Isotope Laboratories) was dried over sodium-benzophenone and distilled under an argon atmosphere. Methanol, ethanol, and 2-propanol (all purchased from Fisher Scientific) were dried over 4 Å molecular sieves and then deoxygenated by bubbling argon through them for one hour. All other dry and oxygen-free solvents used for synthesis and workup (CH_2Cl_2 , *n*-pentane, THF, and toluene, all purchased from Fisher Scientific) were collected from an Innovative Technology solvent purification system. *N*-methyl-2-pyrrolecarboxaldehyde and cyclohexanecarboxaldehyde were purchased from TCI America. Cyclohexanone and cinnamaldehyde were purchased from Fisher Scientific and Eastman Chemical, respectively. All other carbonyl substrates and D_2 (99.8% D) were purchased from Sigma-Aldrich. Prior to use, all liquid aldehydes were freshly distilled under argon and all liquid ketones were deoxygenated by bubbling argon through them for 30 min. $(i\text{PrPN}^{\text{HP}})\text{CuBr}$ (**1a**),¹⁷ $(\text{CyPN}^{\text{HP}})\text{CuBr}$ (**1b**),¹⁸ $(i\text{BuPN}^{\text{HP}})\text{CuBr}$ (**1c**),¹⁸ $i\text{PrPN}^{\text{MeP}}$,⁵² and $(i\text{PrPN}^{\text{HP}})_3\text{Cu}_6\text{H}_6$ (**3a**)¹⁸ were prepared according to literature procedures. Chemical shift values in ^1H and $^{13}\text{C}\{^1\text{H}\}$ NMR spectra were referenced internally to the residual solvent resonances. $^{31}\text{P}\{^1\text{H}\}$ and ^{11}B NMR spectra were referenced externally to 85% H_3PO_4 (0 ppm) and $\text{BF}_3\cdot\text{OEt}_2$ (0 ppm), respectively. Infrared spectra were recorded on a PerkinElmer Spectrum Two FT-IR spectrometer equipped with a smart orbit

diamond attenuated total reflectance (ATR) accessory. High-resolution mass spectrometry data were acquired using a Thermo Scientific LTQ-FT hybrid mass spectrometer.

Synthesis of (^{iPr}PN^HP)Cu(BH₄) (2a). A flame-dried Schlenk flask equipped with a stir bar was charged with **1a** (200 mg, 0.445 mmol) and NaBH₄ (84 mg, 2.22 mmol), and then chilled in an ice bath (0 °C). After slow addition of degassed EtOH (30 mL), the reaction mixture was gradually warmed to room temperature and stirred for 16 h. Removal of the volatiles under vacuum afforded a white solid, which was extracted with toluene (30 mL first and then 5 mL × 3) followed by filtration through Celite to give a colorless solution. Evaporation of the solvent under vacuum and then washing the residue with *n*-pentane (5 mL × 3) afforded the desired product as a white solid (164 mg, 95%). X-ray quality crystals were grown from a toluene/*n*-pentane solution. ¹H NMR (400 MHz, C₆D₆, δ): 2.63-2.41 (m, NCH₂, 4H), 1.83-1.69 (m, PCH(CH₃)₂, 4H), likely 1.56 (q, *J*_{H-B} = 82 Hz, BH₄, 4H), 1.26-1.13 (m, CH(CH₃)₂ + PCH₂, 16H), 1.00-0.83 (m, CH(CH₃)₂, 12H); the NH resonance was not located. ¹H NMR (400 MHz, CD₃OD, δ): 2.96-2.84 (m, NCH₂, 4H), 2.09-1.97 (m, PCH(CH₃)₂, 4H), 1.85-1.72 (m, PCH₂, 4H), 1.30-1.10 (m, CH(CH₃)₂, 24H), 0.71 (q, *J*_{H-B} = 81 Hz, BH₄, 4H); the NH resonance was not located. ¹³C{¹H} NMR (101 MHz, C₆D₆, δ): 44.1 (t, *J*_{C-P} = 2.7 Hz, NCH₂), 24.0 (t, *J*_{C-P} = 9.3 Hz, CH(CH₃)₂), 19.7 (t, *J*_{C-P} = 5.7 Hz, PCH₂), 19.0 (t, *J*_{C-P} = 3.5 Hz, CH(CH₃)₂), 18.2 (t, *J*_{C-P} = 2.2 Hz, CH(CH₃)₂). ³¹P{¹H} NMR (162 MHz, C₆D₆, δ): 2.6 (s). ¹¹B NMR (128 MHz, C₆D₆, δ): -29.0 (quint, *J*_{B-H} = 82.8 Hz). ¹¹B NMR (128 MHz, CD₃OD, δ): -30.9 (quint, *J*_{B-H} = 80.2 Hz). Selected ATR-IR data (solid, cm⁻¹): 3305 (ν_{N-H}), 2952, 2924, 2886, 2866, 2807, 2355 (ν_{B-H}terminal), 2232 (δ_{BH2} overtone), 2020 (ν_{B-H}bridging), 1944, 1458, 1362, 1127 (δ_{BH2}). Anal. Calcd for C₁₆H₄₁BCuNP₂: C, 50.07; H, 10.77; N, 3.65. Found: C, 50.01; H, 10.86; N, 3.59.

Synthesis of (^{Cy}PN^HP)Cu(BH₄) (2b). This compound was obtained as a white solid in 76% yield (0.24 mmol scale reaction) following a procedure similar to that used for **2a**. ¹H NMR (400 MHz, C₆D₆, δ): 2.73-2.53 (m, NCH₂, 4H), 2.08-1.97 (m, 4H), 1.84-1.56 (m, 27H), 1.40-1.28 (m, 10H), 1.25-1.07 (m, CyH, 12H); the NH and BH resonances were not located. ¹³C{¹H} NMR (101 MHz, C₆D₆, δ): 44.5 (s, NCH₂), 33.9 (t, *J*_{C-P} = 8.8 Hz, PCH), 29.0 (s, CyC), 28.8 (s, CyC), 27.5 (t, *J*_{C-P} = 5.9 Hz, CyC), 27.4 (t, *J*_{C-P} = 4.3 Hz, CyC), 26.6 (s, CyC), 20.1 (t, *J*_{C-P} = 5.9 Hz, PCH₂). ³¹P{¹H} NMR (162 MHz, C₆D₆, δ): -6.1 (s). ¹¹B NMR (128 MHz, C₆D₆, δ): -29.8 (br). Selected ATR-IR data (solid, cm⁻¹): 3304 (ν_{N-H}), 2921, 2845, 2802, 2349 (ν_{B-H_{terminal}}), 2338 (ν_{B-H_{terminal}}), 2245 (δ_{BH2} overtone), 2022 (ν_{B-H_{bridging}}), 1946, 1441, 1360, 1134 (δ_{BH2}). Anal. Calcd for C₂₈H₅₇BCuNP₂: C, 61.81; H, 10.56; N, 2.57. Found: C, 61.60; H, 10.53; N, 2.55.

Synthesis of (^{tBu}PN^HP)Cu(BH₄) (2c). This compound was obtained as a white solid in 69% yield (0.50 mmol scale reaction) following a procedure similar to that used for **2a**. X-ray quality crystals were grown from a toluene/*n*-pentane solution. ¹H NMR (400 MHz, C₆D₆, δ): 2.70-2.56 (m, NCH₂, 4H), likely 1.75 (q, *J*_{H-B} = 85 Hz, BH₄, 4H), 1.50-1.38 (m, PCH₂, 4H), 1.36-1.07 (m, C(CH₃)₃, 36H); the NH resonance was not located. ¹³C{¹H} NMR (101 MHz, C₆D₆, δ): 44.5 (s, NCH₂), 33.4 (t, *J*_{C-P} = 5.5 Hz, C(CH₃)₃), 29.7 (t, *J*_{C-P} = 3.8 Hz, C(CH₃)₃), 19.6 (t, *J*_{C-P} = 4.0 Hz, PCH₂). ³¹P{¹H} NMR (162 MHz, C₆D₆, δ): 18.7 (s). ¹¹B NMR (128 MHz, C₆D₆, δ): -27.6 (quint, *J*_{B-H} = 82.3 Hz). Selected ATR-IR data (solid, cm⁻¹): 3299 (ν_{N-H}), 2937, 2895, 2863, 2795, 2353 (ν_{B-H_{terminal}}), 2236 (δ_{BH2} overtone), 2058 (ν_{B-H_{bridging}}), 1969, 1468, 1389, 1363, 1357, 1137 (δ_{BH2}), 1128 (δ_{BH2}). Anal. Calcd for C₂₀H₄₉BCuNP₂: C, 54.61; H, 11.23; N, 3.18. Found: C, 54.47; H, 11.23; N, 3.21.

Synthesis of (^{iPr}PN^{Me}P)CuBr (4a). To an oven-dried Schlenk flask equipped with a stir bar were added ^{iPr}PN^{Me}P (479 mg, 1.50 mmol), CuBr (215 mg, 1.50 mmol), and 20 mL of THF.

The resulting mixture was stirred for 16 h and then filtered through a plug of Celite to give a colorless solution, which was evaporated to dryness under vacuum. The residue was washed with *n*-pentane (10 mL \times 3) and dried under vacuum to afford the desired product as a white solid (590 mg, 85% yield). X-ray quality crystals were grown from a saturated CH₂Cl₂ solution layered with *n*-pentane and kept at -30 °C. ¹H NMR (400 MHz, C₆D₆, δ): 2.25 (s, NCH₃, 3H), 2.13-1.98 (m, 4H), 1.85-1.71 (m, 4H), 1.28-1.20 (m, 4H), 1.19-1.02 (m, CH(CH₃)₂, 24H). ¹³C{¹H} NMR (101 MHz, C₆D₆, δ): 54.5 (t, J_{C-P} = 3.5 Hz, NCH₃), 44.3 (s, NCH₂), 24.2 (t, J_{C-P} = 7.5 Hz, CH(CH₃)₂), 22.2 (t, J_{C-P} = 6.4 Hz, PCH₂), 19.7 (t, J_{C-P} = 2.9 Hz, CH(CH₃)₂), 19.5 (t, J_{C-P} = 3.0 Hz, CH(CH₃)₂). ³¹P{¹H} NMR (162 MHz, C₆D₆, δ): 2.7 (s). Selected ATR-IR data (solid, cm⁻¹): 2953, 2927, 2869, 2822, 2802, 1459, 1238, 1047. Anal. Calcd for C₁₇H₃₉BrCuNP₂: C, 44.11; H, 8.49; N, 3.03. Found: C, 43.86; H, 8.36; N, 3.07.

Representative Procedure for Catalytic Hydrogenation of Aldehydes and Ketones. In a glovebox, an oven-dried Fischer-Porter tube equipped with a stir bar was charged with **1a** (9.0 mg, 0.020 mmol), KO^tBu (0.020 mmol, from a 0.089 M stock solution in THF), and THF to reach a total volume of 3 mL. To the resulting mixture was added 1.0 mmol of the substrate. The sealed tube was taken outside the glovebox and flushed with H₂ three times, after which the H₂ pressure was set to an appropriate value based on the reactivity of the substrate. The reaction was stirred at room temperature for a desired period of time, and then H₂ was vented slowly. An aliquot of the reaction mixture was evaporated and dissolved in CDCl₃ for NMR analysis. The conversion of the substrate was calculated based on the ¹H NMR integrations. Selected alcohol products were subjected to purification on a pipette column packed with silica gel (eluted with a 4 : 1 mixture of EtOAc-hexanes).

Representative Procedure for the Reaction Between 3a and a Carbonyl Substrate. To a dry J. Young NMR tube were added **3a** (3.3 mg, 2.5 μmol), a carbonyl substrate (25 μmol), and ~ 0.3 mL of C_6D_6 . The progress of the reaction (at 23 $^\circ\text{C}$) was periodically monitored by ^1H and $^{31}\text{P}\{^1\text{H}\}$ NMR spectroscopy.

Synthesis of ($^{i\text{Pr}}\text{PN}^{\text{HP}}\text{Cu}(\text{C}_4\text{H}_3\text{NCHO})$) (5a**) from Pyrrole-2-carboxaldehyde.** To an oven-dried Schlenk flask equipped with a stir bar were added **1a** (90 mg, 0.20 mmol), KO^tBu (27 mg, 0.24 mmol), and 10 mL of THF. The resulting mixture was stirred for 2 min, after which pyrrole-2-carboxaldehyde (19 mg, 0.20 mmol) was added. The reaction was kept at room temperature under stirring for 2 h, resulting in a color change from light yellow to orange. The volatiles were removed under vacuum and the residue was extracted with toluene (5 mL \times 3). The combined toluene solutions were concentrated under vacuum, affording the product as an orange-yellow oil (68 mg, 73% yield). Attempts to crystallize the product from *n*-pentane were unsuccessful. ^1H NMR (400 MHz, C_6D_6 , δ): 9.57 (s, CHO, 1 H), 7.48 (s, pyrrole CH, 1H), 7.22 (s, pyrrole CH, 1H), 6.62 (s, pyrrole CH, 1H), 4.12 (br, NH, 1H), 2.66-2.43 (m, 4H), 1.62-1.51 (m, 4H), 1.27-1.29 (m, 4H), 0.95-0.84 (m, $\text{CH}(\text{CH}_3)_2$, 24H). $^{13}\text{C}\{^1\text{H}\}$ NMR (101 MHz, C_6D_6 , δ): 179.3 (s, CHO), 142.5 (s, pyrrole C), 140.3 (s, pyrrole C), 125.2 (s, pyrrole C), 111.9 (s, pyrrole C), 45.2 (s, NCH_2), 24.2 (t, $J_{\text{C-P}} = 6.6$ Hz, $\text{CH}(\text{CH}_3)_2$), 23.2 (t, $J_{\text{C-P}} = 6.3$ Hz, PCH_2), 19.2 (br, $\text{CH}(\text{CH}_3)_2$), 19.0 (br, $\text{CH}(\text{CH}_3)_2$). $^{31}\text{P}\{^1\text{H}\}$ NMR (162 MHz, C_6D_6 , δ): 3.1 (s). Selected ATR-IR data (neat, cm^{-1}): 3243 ($\nu_{\text{N-H}}$), 2952, 2927, 2868, 2754, 2717, 1622 ($\nu_{\text{C=O}}$), 1592, 1461, 1441, 1385, 1364, 1340, 1317. ESI-MS of **5a** in acetonitrile (m/z): [$^{i\text{Pr}}\text{PN}^{\text{HP}}\text{Cu}$] $^+$ calcd for $\text{C}_{16}\text{H}_{37}\text{NP}_2\text{Cu}$ 368.16918, found 368.16908; [$^{i\text{Pr}}\text{PN}^{\text{HP}}\text{Cu} + \text{O}$] $^+$ calcd for $\text{C}_{16}\text{H}_{37}\text{NOP}_2\text{Cu}$ 384.16409, found 384.16413; the parent ion of **5a** was not found.

X-ray Structure Determinations. Crystal data collection and refinement parameters are

provided in the Electronic Supporting Information (ESI). Intensity data were collected at 150 K on a Bruker APEX-II CCD diffractometer using Mo K α radiation, $\lambda = 0.71073 \text{ \AA}$. The data frames were processed using the program SAINT. The data were corrected for decay, Lorentz, and polarization effects as well as absorption and beam corrections based on the multi-scan technique. The structures were solved by a combination of direct methods and the difference Fourier technique as implemented in the SHELX suite of programs and refined by full-matrix least-squares on F^2 . Non-hydrogen atoms were refined with anisotropic displacement parameters. For **2a** and **2c**, hydrogen atoms bound to N and B were located directly from the difference map; the coordinates were refined with the exception of the B-bound hydrogen atoms in **2c**. The B–H hydrogens for **2c** were held fixed at the located positions during the final stage of refinement. All remaining hydrogen atoms were calculated and treated with a riding model. Crystal structures mentioned in this paper have been deposited at the Cambridge Crystallographic Data Centre (CCDC) and allocated the deposition numbers CCDC 2089300-2089302.

CONFLICTS OF INTEREST

There are no conflicts to declare.

ACKNOWLEDGMENTS

We thank the NSF Chemical Catalysis Program (CHE-1464734 and CHE-1800151), the NSF MRI Program (CHE-0215950 for a Bruker APEX-II CCD diffractometer and CHE-1726092 for a Bruker Avance NEO 400 MHz NMR spectrometer), and the University of Cincinnati (Doctoral Enhancement Fellowship to D. A. Ekanayake and A. Chakraborty) for support of this research.

ELECTRONIC SUPPLEMENTARY INFORMATION

Electronic supplementary information (ESI) available: NMR and IR spectra of the copper complexes, and X-ray crystallographic information. CCDC 2089300-2089302. For ESI and crystallographic data in CIF or other electronic format see DOI: 10.1039/xxxxxxxxxx

NOTES AND REFERENCES

- (1) (a) S. Chakraborty and H. Guan, First-Row Transition Metal Catalyzed Reduction of Carbonyl Functionalities: A Mechanistic Perspective, *Dalton Trans.*, 2010, **39**, 7427-7436; (b) S. Chakraborty, P. Bhattacharya, H. Dai and H. Guan, Nickel and Iron Pincer Complexes as Catalysts for the Reduction of Carbonyl Compounds, *Acc. Chem. Res.*, 2015, **48**, 1995-2003; (c) R. J. Trovitch, The Emergence of Manganese-Based Carbonyl Hydrosilylation Catalysts, *Acc. Chem. Res.*, 2017, **50**, 2842-2852; (d) S. R. Tamang and M. Findlater, Emergence and Applications of Base Metals (Fe, Co, and Ni) in Hydroboration and Hydrosilylation, *Molecules*, 2019, **24**, 3194; (e) Á. Raya-Barón, P. Oña-Burgos and I. Fernández, Iron-Catalyzed Homogeneous Hydrosilylation of Ketones and Aldehydes: Advances and Mechanistic Perspective, *ACS Catal.*, 2019, **9**, 5400-5417.
- (2) (a) W. H. Bernskoetter and N. Hazari, Hydrogenation and Dehydrogenation Reactions Catalyzed by Iron Pincer Compounds, in *Pincer Compounds: Chemistry and Applications*, D. Morales-Morales, ed., Elsevier, Amsterdam, 2018, ch. 6, pp. 111-131; (b) W. D. Jones, Hydrogenation/Dehydrogenation of Unsaturated Bonds with Iron Pincer Catalysis, *Top. Organomet. Chem.*, 2019, **63**, 141-174; (c) Z. Wei and H. Jiao, Bifunctional Aliphatic PNP Pincer Catalysts for Hydrogenation: Mechanisms and Scope, *Adv. Inorg. Chem.*, 2019, **73**, 323-384; (d) L. Alig, M. Fritz and S. Schneider, First-Row Transition Metal (De)Hydrogenation Catalysis Based on Functional Pincer Ligands, *Chem. Rev.*, 2019, **119**, 2681-2751; (e) D. A. Ekanayake and H. Guan, Hydrogenation Reactions Catalyzed by PNP-Type Complexes Featuring a $\text{HN}(\text{CH}_2\text{CH}_2\text{PR}_2)_2$ Ligand, *Top. Organomet. Chem.*, 2021, **68**, 263-320.
- (3) (a) P. A. Dub, N. J. Henson, R. L. Martin and J. C. Gordon, Unravelling the Mechanism of the Asymmetric Hydrogenation of Acetophenone by $[\text{RuX}_2(\text{diphosphine})(1,2\text{-diamine})]$ Catalysts, *J. Am. Chem. Soc.*, 2014, **136**, 3505-3521; (b) P. A. Dub and J. C. Gordon, Metal-Ligand Bifunctional Catalysis: The "Accepted" Mechanism, the Issue of Concertedness, and the Function of the Ligand in Catalytic Cycles Involving Hydrogen Atoms, *ACS Catal.*, 2017, **7**, 6635-6655; (c) P. A. Dub and J. C. Gordon, The Role of the Metal-Bound N-H Functionality in Noyori-Type Molecular Catalysts, *Nat. Rev. Chem.*, 2018, **2**, 396-408.
- (4) K. V. Vasudevan, B. L. Scott and S. K. Hanson, Alkene Hydrogenation Catalyzed by Nickel Hydride Complexes of an Aliphatic PNP Pincer Ligand, *Eur. J. Inorg. Chem.*, 2012, 4898-4906.
- (5) (a) W. S. Mahoney, D. M. Brestensky and J. M. Stryker, Selective Hydride-Mediated Conjugate Reduction of α,β -Unsaturated Carbonyl Compounds Using $[(\text{Ph}_3\text{P})\text{CuH}]_6$, *J. Am. Chem. Soc.*, 1988, **110**, 291-293; (b) W. S. Mahoney and J. M. Stryker, Hydride-Mediated Homogeneous Catalysis. Catalytic Reduction of α,β -Unsaturated Ketones Using $[(\text{Ph}_3\text{P})\text{CuH}]_6$ and H_2 , *J. Am. Chem. Soc.*, 1989, **111**, 8818-8823.

- (6) (a) J.-X. Chen, J. F. Daeuble, D. M. Brestensky and J. M. Stryker, Highly Chemoselective Catalytic Hydrogenation of Unsaturated Ketones and Aldehydes to Unsaturated Alcohols Using Phosphine-Stabilized Copper(I) Hydride Complexes, *Tetrahedron*, 2000, **56**, 2153-2166; (b) J.-X. Chen, J. F. Daeuble and J. M. Stryker, Phosphine Effects in the Copper(I) Hydride-Catalyzed Hydrogenation of Ketones and Regioselective 1,2-Reduction of α,β -Unsaturated Ketones and Aldehydes. Hydrogenation of Decalin and Steroidal Ketones and Enones, *Tetrahedron*, 2000, **56**, 2789-2798.
- (7) T. Nakajima, K. Nakamae, Y. Ura and T. Tanase, Multinuclear Copper Hydride Complexes Supported by Polyphosphine Ligands, *Eur. J. Inorg. Chem.*, 2020, 2211-2226.
- (8) C. M. Zall, J. C. Linehan and A. M. Appel, Triphosphine-Ligated Copper Hydrides for CO₂ Hydrogenation: Structure, Reactivity, and Thermodynamic Studies, *J. Am. Chem. Soc.*, 2016, **138**, 9968-9977.
- (9) C. M. Zall, J. C. Linehan and A. M. Appel, A Molecular Copper Catalyst for Hydrogenation of CO₂ to Formate, *ACS Catal.*, 2015, **5**, 5301-5305.
- (10) K. Nakamae, T. Nakajima, Y. Ura, Y. Kitagawa and T. Tanase, Facially Dispersed Polyhydride Cu₉ and Cu₁₆ Clusters Comprising Apex-Truncated Supertetrahedral and Square-Face-Capped Cuboctahedral Copper Frameworks, *Angew. Chem. Int. Ed.*, 2020, **59**, 2262-2267.
- (11) (a) H. Shimizu, D. Igarashi, W. Kuriyama, Y. Yusa, N. Sayo and T. Saito, Asymmetric Hydrogenation of Aryl Ketones Mediated by a Copper Catalyst, *Org. Lett.*, 2007, **9**, 1655-1657; (b) H. Shimizu, T. Nagano, N. Sayo, T. Saito, T. Ohshima and K. Mashima, Asymmetric Hydrogenation of Heteroaromatic Ketones and Cyclic and Acyclic Enones Mediated by Cu(I)-Chiral Diphosphine Catalysts, *Synlett*, 2009, 3143-3146; (c) S. W. Krabbe, M. A. Hatcher, R. K. Bowman, M. B. Mitchell, M. S. McClure and J. S. Johnson, Copper-Catalyzed Asymmetric Hydrogenation of Aryl and Heteroaryl Ketones, *Org. Lett.*, 2013, **15**, 4560-4563; (d) O. V. Zatulochnaya, S. Rodríguez, Y. Zhang, K. S. Lao, S. Tcyrulnikov, G. Li, X.-J. Wang, B. Qu, S. Biswas, H. P. R. Mangunuru, D. Rivalenti, J. D. Sieber, J.-N. Desrosiers, J. C. Leung, N. Grinberg, H. Lee, N. Haddad, N. K. Yee, J. J. Song, M. C. Kozlowski and C. H. Senanayake, Copper-Catalyzed Asymmetric Hydrogenation of 2-Substituted Ketones *via* Dynamic Kinetic Resolution, *Chem. Sci.*, 2018, **9**, 4505-4510; (e) K. Junge, B. Wendt, D. Addis, S. Zhou, S. Das, S. Fleischer and M. Beller, Copper-Catalyzed Enantioselective Hydrogenation of Ketones, *Chem. Eur. J.*, 2011, **17**, 101-105.
- (12) H. Shimizu, N. Sayo and T. Saito, A Practical and Highly Chemoselective Hydrogenation of Aldehydes with a Copper Catalyst, *Synlett*, 2009, 1295-1298.
- (13) R. Watari, Y. Kayaki, S. Hirano, N. Matsumoto and T. Ikariya, Hydrogenation of Carbon Dioxide to Formate Catalyzed by a Copper/1,8-Diazabicyclo[5.4.0]undec-7-ene System, *Adv. Syn. Catal.*, 2015, **357**, 1369-1373.
- (14) H. Liu, Q. Mei, Q. Xu, J. Song, H. Liu and B. Han, Synthesis of Formamides Containing Unsaturated Groups by *N*-Formylation of Amines Using CO₂ with H₂, *Green Chem.*, 2017, **19**, 196-201.
- (15) K. Chaudhary, M. Trivedi, D. T. Masram, A. Kumar, G. Kumar, A. Husain and N. P. Rath, A Highly Active Copper Catalyst for the Hydrogenation of Carbon Dioxide to Formate under Ambient Conditions, *Dalton Trans.*, 2020, **49**, 2994-3000.
- (16) (a) C. Deutsch, N. Krause and B. H. Lipshutz, CuH-Catalyzed Reactions, *Chem. Rev.*, 2008, **108**, 2916-2927; (b) A. J. Jordan, G. Lalic and J. P. Sadighi, Coinage Metal Hydrides: Synthesis, Characterization, and Reactivity, *Chem. Rev.*, 2016, **116**, 8318-8372.

- (17) S. S. Rozenel, J. B. Kerr and J. Arnold, Metal Complexes of Co, Ni and Cu with the Pincer Ligand $\text{HN}(\text{CH}_2\text{CH}_2\text{P}^i\text{Pr}_2)_2$: Preparation, Characterization and Electrochemistry, *Dalton Trans.*, 2011, **40**, 10397-10405.
- (18) D. A. Ekanayake, A. Chakraborty, J. A. Krause and H. Guan, Steric Effects of $\text{HN}(\text{CH}_2\text{CH}_2\text{PR}_2)_2$ on the Nuclearity of Copper Hydrides, *Inorg. Chem.*, 2020, **59**, 12817-12828.
- (19) (a) S. Chakraborty, J. Zhang, Y. J. Patel, J. A. Krause and H. Guan, Pincer-Ligated Nickel Hydridoborate Complexes: the Dormant Species in Catalytic Reduction of Carbon Dioxide with Borane, *Inorg. Chem.*, 2013, **52**, 37-47; (b) S. Qu, H. Dai, Y. Dang, C. Song, Z.-X. Wang and H. Guan, Computational Mechanistic Study of Fe-Catalyzed Hydrogenation of Esters to Alcohols: Improving Catalysis by Accelerating Precatalyst Activation with a Lewis Base, *ACS Catal.*, 2014, **4**, 4377-4388; (c) S. Murugesan, B. Stöger, M. Weil, L. F. Verios and K. Kirchner, Synthesis, Structure, and Reactivity of Co(II) and Ni(II) PCP Pincer Borohydride Complexes, *Organometallics*, 2015, **34**, 1364-1372.
- (20) (a) T. Ohkuma, M. Koizumi, K. Muñiz, G. Hilt, C. Kabuto and R. Noyori, *trans*- $\text{RuH}(\eta^1\text{-BH}_4)(\text{binap})(1,2\text{-diamine})$: A Catalyst for Asymmetric Hydrogenation of Simple Ketones under Base-Free Conditions, *J. Am. Chem. Soc.*, 2002, **124**, 6508-6509; (b) R. Guo, X. Chen, C. Elpelt, D. Song and R. H. Morris, Applications of Ruthenium Hydride Borohydride Complexes Containing Phosphinite and Diamine Ligands to Asymmetric Catalytic Reactions, *Org. Lett.*, 2005, **7**, 1757-1759.
- (21) (a) W. Kuriyama, T. Matsumoto, O. Ogata, Y. Ino, K. Aoki, S. Tanaka, K. Ishida, T. Kobayashi, N. Sayo and T. Saito, Catalytic Hydrogenation of Esters. Development of an Efficient Catalyst and Processes for Synthesising (*R*)-1,2-Propanediol and 2-(*l*-Menthoxy)ethanol, *Org. Process Res. Dev.*, 2012, **16**, 166-171; (b) Z. Han, L. Rong, J. Wu, L. Zhang, Z. Wang and K. Ding, Catalytic Hydrogenation of Cyclic Carbonates: A Practical Approach from CO_2 and Epoxides to Methanol and Diols, *Angew. Chem. Int. Ed.*, 2012, **51**, 13041-13045.
- (22) (a) S. Chakraborty, H. Dai, P. Bhattacharya, N. T. Fairweather, M. S. Gibson, J. A. Krause and H. Guan, Iron-Based Catalysts for the Hydrogenation of Esters to Alcohols, *J. Am. Chem. Soc.*, 2014, **136**, 7869-7872; (b) S. Werkmeister, K. Junge, B. Wendt, E. Alberico, H. Jiao, W. Baumann, H. Jung, F. Gallou and M. Beller, Hydrogenation of Esters to Alcohols with a Well-Defined Iron Complex, *Angew. Chem. Int. Ed.*, 2014, **53**, 8722-8726; (c) S. Elangovan, B. Wendt, C. Topf, S. Bachmann, M. Scalone, A. Spannenberg, H. Jiao, W. Baumann, K. Jung and M. Beller, Improved Second Generation Iron Pincer Complexes for Effective Ester Hydrogenation, *Adv. Synth. Catal.*, 2016, **358**, 820-825; (d) F. Schneck, M. Assmann, M. Balmer, K. Harms and R. Langer, Selective Hydrogenation of Amides to Amines and Alcohols Catalyzed by Improved Iron Pincer Complexes, *Organometallics*, 2016, **35**, 1931-1943; (e) N. M. Rezayee, D. C. Samblanet and M. S. Sanford, Iron-Catalyzed Hydrogenation of Amides to Alcohols and Amines, *ACS Catal.*, 2016, **6**, 6377-6383; (f) M. Garbe, Z. Wei, B. Tannert, A. Spannenberg, H. Jiao, S. Bachmann, M. Scalone, K. Junge and M. Beller, Enantioselective Hydrogenation of Ketones Using Different Metal Complexes with a Chiral PNP Pincer Ligand, *Adv. Synth. Catal.*, 2019, **361**, 1913-1920; (g) H. Dai, W. Li, J. A. Krause and H. Guan, Experimental Evidence of *syn* H–N–Fe–H Configurational Requirement for Iron-Based Bifunctional Hydrogenation Catalysts. *Inorg. Chem.*, 2021, **60**, 6521-6535.

- (23) J. B. Curely, N. E. Smith, W. H. Bernskoetter, N. Hazari and B. Q. Mercado, Catalytic Formic Acid Dehydrogenation and CO₂ Hydrogenation Using Iron PN^{RP} Pincer Complexes with Isonitrile Ligands, *Organometallics*, 2018, **37**, 3846-3853.
- (24) (a) S. J. Lippard and K. M. Melmed, Transition Metal Borohydride Complexes. I. The Structure of Borohydridobis(triphenylphosphine)copper(I), *J. Am. Chem. Soc.*, 1967, **89**, 3929-3930; (b) S. J. Lippard and D. A. Ucko, Transition Metal Borohydride Complexes. II. The Reaction of Copper(I) Compounds with Boron Hydride Anions, *Inorg. Chem.*, 1968, **7**, 1051-1056; (c) B. E. Green, C. H. L. Kennard, G. Smith, M. M. Elcombe, F. H. Moore, B. D. James and A. H. White, Crystal Structures of α - and β -(1,10-Phenanthroline)tetrahydroborato(triphenylphosphine)copper(I) and (2,9-Dimethyl-4,7-diphenyl-1,10-phenanthroline)tetrahydroboratocopper(I), *Inorg. Chim. Acta*, 1984, **83**, 177-189; (d) M. Lueckheide, N. Rothman, B. Ko and J. M. Tanski, π -Stacking Motifs in the Crystal Structures of Bis(phosphine) Copper(I) η^2 -Tetrahydroborate Complexes, *Polyhedron*, 2013, **58**, 79-84; (e) X. Hu, M. Soleihavoup, M. Melaimi, J. Chu and G. Bertrand, Air-Stable (CAAC)CuCl and (CAAC)CuBH₄ Complexes as Catalysts for the Hydrolytic Dehydrogenation of BH₃NH₃, *Angew. Chem. Int. Ed.*, 2015, **54**, 6008-6011; (f) N. V. Belkova, I. E. Golub, E. I. Gutsul, K. A. Lyssenko, A. S. Peregudov, V. D. Makhaev, O. A. Filippov, L. M. Epstein, A. Rossin, M. Peruzzini and E. S. Shubina, Binuclear Copper(I) Borohydride Complex Containing Bridging Bis(diphenylphosphino) Methane Ligands: Polymorphic Structures of $[(\mu_2\text{-dppm})_2\text{Cu}_2(\eta^2\text{-BH}_4)_2]$ Dichloromethane Solvate, *Crystals*, 2017, **7**, 318.
- (25) G. F. Svatos, C. Curran and J. V. Quagliano, Infrared Absorption Spectra of Inorganic Coordination Complexes. V. The N-H Stretching Vibration in Coordination Compounds, *J. Am. Chem. Soc.*, 1955, **77**, 6159-6163.
- (26) J. Joseph and E. D. Jemmis, Red-, Blue-, or No-Shift in Hydrogen Bonds: A Unified Explanation, *J. Am. Chem. Soc.*, 2007, **129**, 4620-4632.
- (27) T. Seki, T. Nakajo and M. Onaka, The Tishchenko Reaction: A Classic and Practical Tool for Ester Synthesis, *Chem. Lett.*, 2006, **35**, 824-829.
- (28) W. D. Phillips, H. C. Miller and E. L. Muetterties, B¹¹ Magnetic Resonance Study of Boron Compounds, *J. Am. Chem. Soc.*, 1959, **81**, 4496-4500.
- (29) (a) T. H. Lemmen, K. Folting, J. C. Huffman and K. G. Caulton, Copper Polyhydrides, *J. Am. Chem. Soc.*, 1985, **107**, 7774-7775; (b) D. M. Brestensky, D. E. Huseland, C. McGettigan and J. M. Stryker, Simplified, "One-Pot" Procedure for the Synthesis of $[(\text{Ph}_3\text{P})\text{CuH}]_6$, a Stable Copper Hydride for Conjugate Reductions, *Tetrahedron Lett.*, 1988, **29**, 3749-3752.
- (30) K. Azizi and R. Madsen, Radical Condensation Between Benzylic Alcohols and Acetamides to Form 3-Arylpropanamides. *Chem. Sci.*, 2020, **11**, 7800-7806.
- (31) N. A. Eberhardt, N. P. N. Wellala, Y. Li, J. A. Krause and H. Guan, Dehydrogenative Coupling of Aldehydes with Alcohols Catalyzed by a Nickel Hydride Complex, *Organometallics*, 2019, **38**, 1468-1478.
- (32) (a) Y. Watanabe, K. Sawada and M. Hayashi, A Green Method for the Self-Aldol Condensation of Aldehydes Using Lysine, *Green Chem.*, 2010, **12**, 384-386; (b) L. K. Sharma, K. B. Kim and G. I. Elliott, A Selective Solvent-Free Self-Condensation of Carbonyl Compounds Utilizing Microwave Irradiation, *Green Chem.*, 2011, **13**, 1546-1549.
- (33) Both GC-MS and NMR could confirm the allylic alcohol product; however, a number of other unidentified products were also present, possibly resulting from various enolate

- addition reactions. Compared to the Stryker's catalyst, the $^{\text{R}}\text{PN}^{\text{HP}}$ -ligated copper system reported here may be more basic, promoting enolate chemistry.
- (34) (a) D. M. L. Goodgame and F. A. Cotton, Phosphine Oxide Complexes. Part IV. Tetrahedral, Planar, and Binuclear Complexes of Copper(II) with Phosphine Oxides, and Some Arsine Oxide Analogues, *J. Chem. Soc.*, 1961, 2298-2305; (b) G. Pilloni, G. Valle, C. Corvaja, B. Longato and B. Corain, Copper(II) and Copper(I) Complexes Stabilized by Phosphine Oxides: Synthesis and Characterization of the Cationic Complexes $[\text{Cu}(\text{odppf})_2(\text{EtOH})]^{2+}$ and $[\text{Cu}(\text{odppf})_2]^{2+}$, Precursors of the Novel Copper(I) Adduct $[\text{Cu}(\text{odppf})_2]^+$ (odppf = 1,1'-Bis(oxodiphenylphosphoranyl)ferrocene). Crystal Structure of $[\text{Cu}(\text{odppf})_2(\text{EtOH})](\text{BF}_4)_2$ and $[\text{Cu}(\text{odppf})_2](\text{BF}_4)_2$, *Inorg. Chem.*, 1995, **34**, 5910-5918.
- (35) Though we do not have evidence supporting that $(^{\text{iPr}}\text{PN}^{\text{HP}})_n\text{Cu}_n\text{H}_n$ ($n = 1-3$) exist, structures of $(\kappa^2\text{-triphos})_2\text{Cu}_2\text{H}_2$, $[(S)\text{-SEGPHOS}]_2\text{Cu}_2\text{H}_2$ ($(S)\text{-SEGPHOS}$ is a chiral diphosphine), and $(\text{dppbz})_3\text{Cu}_3\text{H}_3$ (dppbz = 1,2-bis(diphenylphosphino)benzene) have been reported. For details, see: (a) G. V. Goeden, J. C. Huffman and K. G. Caulton, A Cu-(μ -H) Bond Can Be Stronger Than an Intramolecular P \rightarrow Cu Bond. Synthesis and Structure of $\text{Cu}_2(\mu\text{-H})_2[\eta^2\text{-CH}_3\text{C}(\text{CH}_2\text{PPh}_2)_3]_2$, *Inorg. Chem.*, 1986, **25**, 2484-2485; (b) Y. Xi and J. F. Hartwig, Mechanistic Studies of Copper-Catalyzed Asymmetric Hydroboration of Alkenes, *J. Am. Chem. Soc.*, 2017, **139**, 12758-12772; (c) M. S. Eberhart, J. R. Norton, A. Zuzek, W. Sattler and S. Rucolo, Electron Transfer from Hexameric Copper Hydrides, *J. Am. Chem. Soc.*, 2013, **135**, 17262-17265.
- (36) N. P. Fitzsimons, W. Jones and P. J. Herley, Studies of Copper Hydride. Part 1. – Synthesis and Solid-State Stability, *J. Chem. Soc., Faraday Trans.*, 1995, **91**, 713-718.
- (37) P. A. Dub, B. L. Scott and J. C. Gordon, Why Does Alkylation of the N–H Functionality within M/NH Bifunctional Noyori-Type Catalysts Lead to Turnover? *J. Am. Chem. Soc.*, 2017, **139**, 1245-1260.
- (38) (a) Y. Zhang, A. D. MacIntosh, J. L. Wong, E. A. Bielinski, P. G. Williard, B. Q. Mercado, N. Hazari, and W. H. Bernskoetter, Iron Catalyzed CO_2 Hydrogenation to Formate Enhanced by Lewis Acid Co-Catalysts, *Chem. Sci.*, 2015, **6**, 4291-4299; (b) J. Yuwen, S. Chakraborty, W. W. Brennessel and W. D. Jones, Additive-Free Cobalt-Catalyzed Hydrogenation of Esters to Alcohols, *ACS Catal.*, 2017, **7**, 3735-3740; (c) U. Jayarathne, N. Hazari and W. H. Bernskoetter, Selective Iron-Catalyzed N -Formylation of Amines Using Dihydrogen and Carbon Dioxide, *ACS Catal.*, 2018, **8**, 1338-1345.
- (39) Because nitrogen and phosphorus are separated by two carbon atoms, the electronic and steric effects of NH vs. N -alkyl on the phosphorus donor ability should be similar.
- (40) L. Yang, D. R. Powell and R. P. Houser, Structural Variation in Copper(I) Complexes with Pyridylmethylamide Ligands: Structural Analysis with a New Four-Coordinate Geometry Index, τ_4 , *Dalton Trans.*, 2007, 955-964.
- (41) T-shaped Cu(I) complexes supported a PNP pincer ligand are known in the literature, although the central donor is pyridine-based. For examples, see: (a) J. I. van der Vlugt, E. A. Pidko, D. Vogt, M. Lutz, A. L. Spek and A. Meetsma, T-Shaped Cationic Cu^{I} Complexes with Hemilabile PNP-Type Ligands, *Inorg. Chem.*, 2008, **47**, 4442-4444; (b) J. I. van der Vlugt, E. A. Pidko, D. Vogt, M. Lutz and A. L. Spek, Cu^{I} Complexes with a Noninnocent PNP Ligand: Selective Dearomatization and Electrophilic Addition Reactivity, *Inorg. Chem.*, 2009, **48**, 7513-7515; (c) K. Takeuchi, Y. Tanaka, I. Tanigawa, F. Ozawa and J.-C. Choi, Cu(I) Complex Bearing a PNP-Pincer-Type Phosphaalkene Ligand with a Bulky

- Fused-Ring Eind Group: Properties and Applications to FLP-Type Bond Activation and Catalytic CO₂ Reduction, *Dalton Trans.*, 2020, **49**, 3630-3637.
- (42) G. V. Goeden and K. G. Caulton, Soluble Copper Hydrides: Solution Behavior and Reactions Related to CO Hydrogenation, *J. Am. Chem. Soc.*, 1981, **103**, 7354-7355.
- (43) O. G. Shirobokov, L. G. Kuzmina and G. I. Nikonov, Nonhydride Mechanism of Metal-Catalyzed Hydrosilylation, *J. Am. Chem. Soc.*, 2011, **133**, 6487-6489.
- (44) B. L. Tran, B. D. Neisen, A. L. Speelman, T. Gunasekara, E. S. Wiedner and R. M. Bullock, Mechanistic Studies on the Insertion of Carbonyl Substrates into Cu-H: Different Rate-Limiting Steps as a Functional of Electrophilicity, *Angew. Chem. Int. Ed.*, 2020, **59**, 8645-8653.
- (45) G. Xu, S. Leloux, P. Zhang, J. Meijide Suárez, Y. Zhang, E. Derat, M. Ménand, O. Bistri-Aslanoff, S. Roland, T. Leysens, O. Riant and M. Sollogoub, Capturing the Monomeric (L)CuH in NHC-Capped Cyclodextrin: Cavity-Controlled Chemoselective Hydrosilylation of α,β -Unsaturated Ketones, *Angew. Chem. Int. Ed.*, 2020, **59**, 7591-7597.
- (46) The chemical shift value for the NH resonance (4.12 ppm) and the broadening of the NH stretching band suggest some weak HBI between the NH group and the oxygen atom of the carbonyl group. For a reference to varying degrees of HBIs in ⁱPrPN^HP-ligated metal complexes, see: N. P. N. Wellala, J. D. Luebking, J. A. Krause and H. Guan, Roles of Hydrogen Bonding in Proton Transfer to $\kappa^P, \kappa^P, \kappa^P$ -N(CH₂CH₂PⁱPr₂)₂-Ligated Nickel Pincer Complexes, *ACS Omega*, 2018, **3**, 4986-5001.
- (47) We also examined the reduction of 4-(trifluoromethyl)benzaldehyde, *o*-tolualdehyde, and 2-fluorobenzaldehyde with **3a**, which all yielded the expected insertion products.
- (48) G. M. Whitesides, J. S. Sadowski and J. Lilburn, Copper(I) Alkoxide. Synthesis, Reactions, and Thermal Decomposition, *J. Am. Chem. Soc.*, 1974, **96**, 2829-2835.
- (49) We cannot rule out the possibility that the carbonyl insertion step takes place on (RⁿPN^HP)_nCu_nH_n or (RⁿPN^HP)_nCu_{2n}H_{2n} (n = 2, 3) whereas regeneration of the hydride from the copper alkoxide intermediate involves a mononuclear species with NH coordination. If this holds true, a significant NH effect could also be observed.
- (50) In principle, the hydrogenolysis and cooperative elimination mechanisms can be differentiated by tracking deuterium during a stoichiometric reaction between (ⁱPrPN^DP)CuH (generated from (ⁱPrPN^DP)CuBr or (ⁱPrPN^DP)₃Cu₆H₆) and a carbonyl substrate. Such an effort was discouraged by the fact that (ⁱPrPN^HP)CuBr and (ⁱPrPN^HP)₃Cu₆H₆ undergo rapid H/D exchange between the NH hydrogen and deuterated alcohols (CD₃OD or ^tBuOD).
- (51) The solution color during ketone hydrogenation (catalyzed by **1a**-KO^tBu) is noticeably darker than the color observed during aldehyde hydrogenation, hinting that a higher percentage of the copper hydride is in the cluster form.
- (52) S. Werkmeister, K. Junge, B. Wendt, E. Alberico, H. Jiao, W. Baumann, H. Jung, F. Gallou and M. Beller, Hydrogenation of Esters to Alcohols with a Well-Defined Iron Complex, *Angew. Chem. Int. Ed.*, 2014, **53**, 8722-8726.